CATHODE-RAY OSCILLOSCOPIC INVESTIGATION OF PHENOMENA AT POLARIZABLE MERCURY ELECTRODES

J. WEST LOVELAND AND PHILIP J. ELVING

Department of Chemistry, The Pennsylvania State College, State College, Pennsylvania

Received August 21, 1951

CONTENTS

I. Introduction

The present review is intended to be a critical summary and evaluation of the use which can be made of recording by the cathode-ray oscillograph in the study of phenomena occurring at the interface between a mercury electrode and the solution in contact with the electrode. These phenomena involve both energy (thermodynamic) and rate (kinetic) factors, and are suitable subjects for investigation as a means of elucidating the rate and mechanism of electrode reactions and the general nature of reversible and irreversible reactions.

The study of mercury electrodes, as compared to that of other metal electrodes, has the advantage that a constant reproducible electrode is assured whose past history—chemical, electrical, and metallurgical—will play no part in the observed phenomena.

The development of the technique of cathode-ray oscilloscopic observation of phenomena at mercury electrodes has been intimately connected in recent years with the development of polarography.

The basic principle of polarography as originated by Heyrovsky in the early twenties (52) is the measurement of the diffusion current passed by a dropping mercury microelectrode in a state of concentration polarization. The rate of diffusion attains a constant value, which is directly proportional to the concentration of the electroactive species in the bulk of the solution; hence the diffusion current is directly proportional to the concentration in the body of the solution. A complete quantitative-qualitative relationship is obtained from a plot of current *vs.* potential. The time required to secure a polarogram with ordinary apparatus is 10 min. or more. The literature on the theory and application of the polarographic technique has been classified in recent bibliographies (55).

During the past ten years numerous papers have appeared, demonstrating the application of the cathode-ray oscilloscope to the recording of polarographic phenomena. Polarographic oscillograms may be obtained in the matter of a few seconds. The information obtainable from them is comparable to and, in many cases, greater than that obtainable from ordinary polarograms. Recently developed techniques offer a rapid and accurate means of obtaining on the screen of a cathode-ray oscilloscope records of capacity-current data, of the differential

capacity of the electrical double layer, and of interfacial phenomena; such observations can be used to study film formation at the interface.

The most comprehensive review to date has been that of Laitinen (54), which is largely restricted to aspects related to the kinetics of electrode processes. Oscillographic and alternating-current polarography are discussed. The implications of the oscillographic approach are less thoroughly considered than are some of the results obtained. Although Laitinen's review was published in 1950, only four papers dealing with oscillographic polarography, published subsequent to 1947, are discussed.

The purpose of the present review is to discuss the theory, experimental principles, applications, and results of the application of oscillographic recording to phenomena at polarized mercury electrodes, including oscillographic polarography.

II. General Discussion

The terms "voltage" and "potential" will be used frequently throughout this article; to avoid ambiguity in usage, the present authors have adopted the following more or less arbitrary terminology. By the term "voltage" is meant "applied electromotive force" (E.M.F.), which is a directly measured quantity. On the other hand, the term "potential" refers to a single electrode; hence "potential difference" is always associated with two electrodes. The term "potential," as commonly used, refers to the state of an electrode compared to some standard electrode; the saturated calomel electrode is the standard electrode implied in the subsequent discussion unless otherwise indicated. Where no current flows between two electrodes, the applied electromotive force is identical with the potential difference of the two electrodes. If current does flow, then the applied voltage differs from the potential difference by an amount depending on the product of the current flowing and the combined resistances of the cell. The latter may be considered as including certain overvoltage effects.

A. Rate of Potential Variation

In ordinary polarography, the voltage applied to the dropping mercury electrode is increased slowly at a rate which usually does not exceed 0.005 v. per second over a span of about 2 v. This voltage variation is sufficiently slow to allow for a steady increase in diffusion current to a constant limiting value. The theory of the diffusion current is discussed in standard references on polarography (35, 52). The original Ilkovic equation defining the diffusion current has been modified in recent years (58, 63, 77).

In oscillographic polarography, i.e., the recording of polarographic phenomena on the cathode-ray oscilloscope, at moderately slow voltage sweeps, e.g., 10 cycles per second (c.p.s.), the voltage variation is 20 v. per second for the same 2-v. span. Such a rapid change in voltage causes the diffusion current passed by the microelectrode to vary with time (70). Figure 1A shows the variation of concentration of the reducible species with the distance from the electrode at different time intervals, t, of electrolysis, where t for each curve is arbitrarily

taken on a basis of $t = 1$. The distance a to b is that distance from the electrode within which all species reducible at the applied voltage react at the electrode. The points of intersection of line b-b' with the various time curves are used for plotting the variation of concentration at the electrode with time (figure 1B). Since the current which passes through the mercury microelectrode is proportional to the concentration of the reducible species around it, i.e., within the distance a to b, the current will vary in the same manner with time. Thus, when a rapid voltage sweep is applied to the dropping mercury electrode, the half-wave potential of the reducible ion will be surpassed so quickly that there will not be sufficient time for the limiting current to attain its constant value, as in ordinary polarography. Instead, once the half-wave potential has been surpassed, as the voltage continues to increase with time, the current continues to decrease with time according to figure 1B. As a result, the typical oscillographic pattern for the current–potential relationship will look somewhat like that in figure 1C. The current rises to a maximum value, then decreases as the diffusion

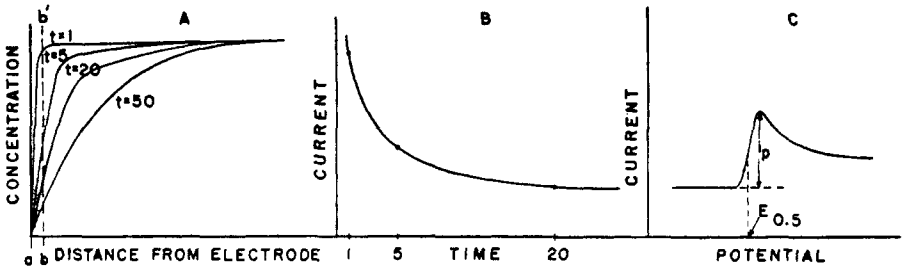

FIG. 1. Relations at a mercury electrode: (A) variation of the concentration of a reducible species about the surface of a mercury electrode at various time intervals; (B) variation of diffusion current at a mercury electrode as a function of time; (C) current–potential relationship under oscillographic conditions.

layer widens, and finally levels off as the limiting current is approached. The peak-current value, p or i_p, is several times greater than the diffusion current observed in ordinary polarographic studies and is a function of the square root of the rate of potential variation.

B. CAPACITY-CURRENT PHENOMENA

Oscillographic polarography differs from classical polarography in another aspect. Because of the large capacity of the electrical double layer between the surface of the dropping mercury electrode and the solution, and the rapid change of potential used in oscillographic work, a capacity current of large magnitude is produced, which cannot be neglected. In studies of depolarization processes, the total current consists of the capacity current and the diffusion current. For cases where the depolarizer is present in dilute quantities, e.g., 10^{-5} N, the capacity current becomes of the same order of magnitude as the diffusion current and the current–potential oscillogram is distorted.[1]

[1] Distortion of the current–potential oscillograms is greatest for ions which are reduced near the potential of the electrocapillary maximum and at potentials more positive than

Both the capacity current and the diffusion current increase considerably during the growth of a mercury drop. As a result of this increase in the size of the mercury drop with time, the observed oscillograms are not steady, but vary in accordance with the area of the drop, making quantitative measurements difficult. The general procedure is to measure the diffusion current when the drop is at its maximum size, prior to dropping off. Another method is to use a delayed voltage sweep, so synchronized with the drop of mercury that the sweep comes at a definite age and hence, probably, area of the drop. Steady oscillograms, however, may be obtained by employing a streaming mercury electrode (38, 41, 47). In this case, a jet of mercury streams upward from a capillary at an angle of about 45 degrees through about 5 mm. of solution. This method provides a constant area of mercury surface in contact with the solution. The amount of solution which the streaming mercury electrode carries along with it is difficult to ascertain, so that the actual exposed area of mercury, although constant, may be calculated only roughly.

The currents passed by the polarographic cell in oscillographic observation are much greater (10 to 100 times) than those found in ordinary polarography. The supporting electrolyte should be fairly concentrated, e.g., 1 N, and the electrodes kept very near to each other, in order to minimize as much as possible the iR drop through the solution. Whereas the resistance of the capillary of mercury in the electrode is ordinarily negligible, a resistance of 100 ohms or so in oscillographic work becomes somewhat appreciable. A low-resistance dropping mercury electrode may be made without altering any of its characteristics by inserting a platinum electrode into the capillary bore near the tip of the capillary (59).

C. FUNDAMENTAL EXPERIMENTAL CIRCUITS

Basically, the conventional polarographic circuit is used in oscillographic polarography. A source of variable E.M.F. must be supplied to the polarographic cell to effect electrolysis; the current passed by the cell is measured by registering the voltage drop (iR) which it makes across a resistor in series with the cell. However, the usual battery–potentiometer source of E.M.F. is supplanted by an electronic voltage-sweep generator. The generated voltage sweep or one synchronized with it is used for deflecting the electron beam of the cathode-ray oscilloscope horizontally after being amplified either by the amplifiers supplied within the oscilloscope or by external amplifiers or by both. The iR drop of the series current-measuring resistor is applied to the vertical deflection plates of the oscilloscope after similar amplification. The basic circuit usually employed may be represented by a block diagram (figure 2), where R is the current-measuring resistance and C is the polarographic cell.

When the voltage sweep is linear, the rate of change of voltage with time (dE/dt) is constant and the rate of progression of the horizontal sweep is proportional to the voltage applied to the cell. The vertical deflection is an indica-

---

the electrocapillary maximum potential, since the capacity of the electrical double layer varies the greatest with potential in this region.

tion of the iR drop of the current-measuring resistor and is proportional to the current passed by the cell. The trace obtained on the oscilloscope is therefore an i–E polarogram and may appropriately be called an oscillographic polarogram.

By a different experimental circuit, a potential–time (E–t) curve may be obtained with an oscilloscope. For producing an E–t trace, a sine wave is applied to a polarographic cell through a large resistance, resulting in a constant current flow through the polarographic cell. The voltage impressed across the cell is amplified and placed on the vertical deflection plates of the cathode-ray oscilloscope. The frequency of the horizontal time sweep is synchronized with that of the applied alternating voltage. Consequently, the vertical deflection is a function of the potential of the cell, the horizontal deflection is proportional to time, and the pattern obtained has a potential–time relationship. When depolarizers are present in a solution a time-lag occurs, as evidenced by a kink in the trace at the reduction or oxidation potential of the depolarizer. By placing a resistance–capacitance differentiating circuit across the cell, the first deriva-

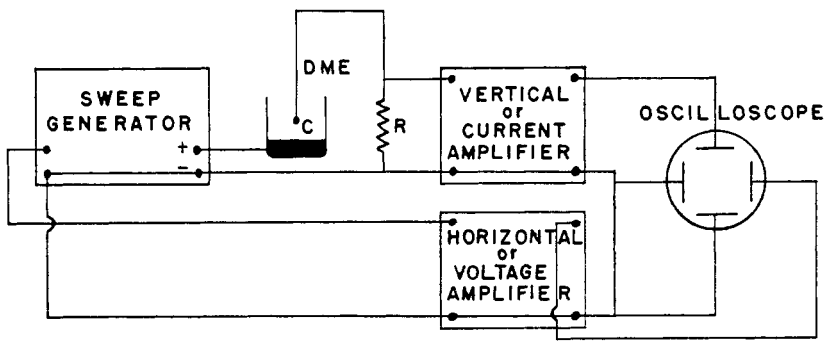

FIG. 2. Block diagram for an oscillographic apparatus for the observation of phenomena at a mercury electrode.

tive of the potential–time curve may be obtained. The effect of this is to accentuate any time-lag, so that even the slightest change in the slope of the E–t curve is easily detected.

D. APPLICABILITY

Although the cathode-ray oscilloscope has been applied to electrode investigations, such as the measurement of phenomena at nickel and copper electrodes, this review will cover only the techniques applied to mercury electrodes and the various interpretations obtained with them. The readily and rapidly reproducible nature of a mercury electrode makes it unique among metallic electrodes in the avoidance of effects associated with the previous history, metallurgical and otherwise, of the electrode.

Perhaps the most significant feature of oscillographic observation is its ability to discriminate between fast and slow rates of reaction at the mercury electrode and to give information concerning the reversibility of electrode processes. When the electrode process is very rapid, only the rate of diffusion governs the

current, but when the rate of reaction is slow, diffusion becomes of secondary importance and the maximal current is a function of the kinetics of the reaction. Rapid kinetic processes at the dropping mercury electrode give rise to a peak current, as outlined subsequently (figure 13A). Slow kinetic processes are characterized by flatter, more rounded peaks and in some cases by a mere rise in current to a constant value (figure 13C). The rapid-rate electrode processes are usually associated with reversible processes, although this need not always be true; e.g., zinc ion reacts fairly rapidly at the electrode but is quite irreversible in nature, at least as far as oscillographic observation is concerned.

Oscillographic polarography is well adapted to following rapid reactions in solution in which one or more of the reacting species is reducible. This technique has been investigated only recently and should prove in the future to be one of the more valuable tools for following fast reactions in solution.

Adsorption phenomena at the mercury electrode have been effectively studied by observing current–time oscillograms for individual drops. Adsorption of a chemical species usually is characterized by maxima in the current–time curves. Current–potential curves have been used as well to investigate adsorption phenomena. The data obtained by such techniques provide clues to a better understanding of many irreversible electrode reactions.

The study of the capacitive properties of the interfacial region by the oscillographic approach offers a new tool for the investigation of the phenomena which are involved in film formation at the interface as well as for the investigation of the nature of electron transfer between the electrode and a species from the solution. For example, it may be possible to determine whether or not electron transfer is preceded by adsorption of the electroactive species on the surface of the electrode.

Also described in the literature are methods for the direct determination of half-wave potentials in connection with the cathode-ray oscilloscope. In yet another technique, the oscilloscope has functioned as an ammeter for studying the variation of current during the formation of a mercury drop.

Reviews on oscillographic polarography in the literature (49, 50, 54, 56, 57, 65) have tended to emphasize a specific part of the field, such as instrumentation, or to cover only a few of the oscillographic circuits and their applications. The present authors hope to give a more complete presentation of the field of oscillographic polarography and related subjects, as well as of the general area involving mercury electrodes.

III. Theoretical Relations and Equations

A. DIFFUSION-CURRENT PROCESSES

1. Proposed equations

Several attempts have been made to develop an equation for the diffusion current at a dropping mercury electrode in oscillographic polarography. Ilkovic's equation (52) for diffusion currents at a dropping mercury electrode for ordinary polarography has been established for several years:

$$i_d = 0.00732FnCD^{1/2}m^{2/3}t^{1/6}$$

where i_d = the maximum current in microamperes at 25°C.,
F = the Faraday (96,500 coulombs),
n = the number of electrons transferred per molecule of electroactive species,
C = the concentration of the electroactive species in millimoles per liter,
D = the diffusion coefficient of the electroactive species in centimeters squared per second,
m = the average mass of mercury flowing in milligrams per second,
t = the life-time of the drop in seconds, and
0.00732 = factors of geometry, π, density of mercury, etc.

The adequacy of the Ilkovic equation has been discussed by Lingane and others (58, 77). More exact forms, which involve a correction factor for the curvature of the drop, have been proposed. Studies of the variation of the diffusion current with time indicate that either $i_d = kt^{1/3}$ (62) or $i_d = kt^{0.249}$ (78) fits the experimental data better than the expression $i_d = kt^{1/6}$, given by the Ilkovic equation, during the early life of the drop.

Thus far there has been only fair agreement in the equations derived for the diffusion current in oscillographic methods of measurement. Randles (72) and Sevcik (74) independently developed theoretical equations for the current given by the current–potential curves obtained in oscillographic polarography. Randles defines the boundary conditions at the mercury–solution interface by the equation

$$\frac{0.059}{n} \log (C_A/C_S) = a(t - t_0) \tag{2}$$

where C_A is the concentration of the metal in the mercury, C_S is the concentration of the metal ions in solution, n is the number of electrons involved in the reaction, a is the rate of change of voltage, t is time in seconds with respect to t_0, and t_0 is the time at which C_A equals C_S. The problem was to solve the diffusion current equation (52, page 18) for linear diffusion towards a plane surface, using the boundary conditions at the interface as defined by equation 2. By using a graphical method based on the numerical solution of differential equations employing small differences, Randles obtained the diffusion-current equation for the case where the electrode reaction occurs reversibly and the reactants and products are soluble either in the aqueous medium or in the electrode material. The equation is

$$i_p = \frac{1.24FCm}{(0.0118)^{1/2}10^3} \gamma^{2/3} t_p^{2/3} n^{3/2} a^{1/2} D^{1/2} \text{ amperes} \tag{3}$$

where i_p = the peak value of the current (amperes),
t_p = the time at which the peak occurs from the beginning of the drop-life,
a = the rate of potential change in volts per second,

C_m = the concentration of the reducible species in moles per cubic centimeter,

γ = a constant depending on the rate of flow of the mercury,

and F, D, and n have the same meanings as before.

Evaluating some of the terms of equation 3 and converting it into a form similar to equation 1 gives

$$i_p = 0.0242Fn^{3/2}CD^{1/2}m^{2/3}t_p^{2/3}v^{1/2} \text{ microamperes} \tag{4}$$

where v is the rate of potential change in volts per second.

Sevcik (74), using essentially the same boundary conditions as Randles, solved the linear diffusion equation by the intuitive method as well as by the application of the operator calculus. The diffusion-current equation is:

$$I_{max} = nFqD^{1/2}(nFg/RT)^{1/2}\ 0.361\ \theta \text{ amperes} \tag{5}$$

Simplifying,

$$I_{max} = Kn^{3/2}F^{3/2}g^{1/2}D^{1/2}C \text{ amperes} \tag{6}$$

where K = the constants q, 0.361, θ, and $(RT)^{-1/2}$,

q = an electrical surface factor or area,

g = the rate of change of voltage in volts per second,

θ = a constant, 1 second$^{1/2}$,

R = the gas constant (joules), and

T = the absolute temperature.

Converting to a form similar to equation 1 gives:

$$i_{max} = 0.0191Fn^{3/2}CD^{1/2}m^{2/3}t^{2/3}v^{1/2} \text{ microamperes} \tag{7}$$

2. Verification and criticism of proposed equations

Comparison of equations 4 and 7 indicates their identity except for a 23 per cent difference in numerical constants. Comparison of either equation 4 or 7 with equation 1 indicates differences in form by factors of the square roots of n, t, and v. When $v = 0$, equations 4 and 7 predict that the diffusion current will be zero. This is not strictly true if the applied potential is more negative than the reduction potential of the reducible species. In this case a small diffusion current will flow, which is given by the Ilkovic equation. Combining equations 1 and 4, the total peak current is equal to the following:

$$i_p = FnCD^{1/2}m^{2/3}t_p^{1/6}(0.00732 + 0.0242n^{1/2}t_p^{1/2}v^{1/2}) \tag{8}$$

Direct experimental verification of equation 8 is lacking. However, a test of the equation may be had by the use of data available in determining the variation of the peak current with change in experimental conditions.

(a) Rate of potential variation

Randles (72) has calculated the ratio of $(i_p/v^{1/2})$ for a solution containing 0.25 millimole of thallium at various values of v. In general, the values of the ratio

decrease as v increases. Designating the theoretical current obtained from equation 1 as i_d and calculating the ratio of $(i_p - i_d)/v^{1/2}$, one finds that the ratio increases in numerical value as v increases. When the ratio of $(i_p - 0.5i_d)/v^{1/2}$ is used, then the ratio varies about a mean value as v increases, signifying that a constant current of about half the magnitude given by the Ilkovic equation should be considered. In the case of 0.25 millimole of cadmium, the ratio of $(i_p/v^{1/2})$ decreases a lesser amount as v increases than in the case of thallium. The ratio which best fits the data is $(i_p - (<0.5i_d))/v^{1/2}$. From the data on cobalt, it is apparent that the contribution to the total peak current of the current from the Ilkovic equation in equation 8 is larger than that required to satisfy the ratio test. To fit Randles' data, equation 8 may be rewritten as

$$i_p = FnCD^{1/2}m^{2/3}t_p^{1/6}(0.00732K + 0.0242n^{1/2}t_p^{1/2}v^{1/2}) \qquad (9)$$

where K is some characteristic fraction for a particular species.

Sevcik (74) has also studied the relationship between peak current and the square root of frequency for various drop-times and various depolarizers. The drop-times and depolarizers were not stated. The frequencies used were 0.794, 3.55, 20.8, and 73.4 cycles per second. Plots of maximal peak current *vs.* square root of frequency which Sevcik obtained for the four cases investigated are straight lines which, when extrapolated, pass through the origin. A critical observation of the graph shows that all the points obtained at a frequency of 3.55 cycles per second for each curve are conspicuously higher than the lines drawn. Other points have a general tendency to lie slightly above the drawn lines. If the straight lines were redrawn according to these tendencies, they would cut the current axis just above the origin. The small positive current represented by the point where the proposed line crosses the current axis is in accordance with equation 9.

Delahay (14) has experimentally tested the relationship of peak current to the square root of the rate of potential change for zinc ion at three different concentrations (1, 0.5, and 0.2 millimolar). The expected straight-line plot is only partially realized in all three cases; the curves are straight for the lower rates of potential variation but tend to deviate at higher rates of potential variation in a manner which decreases the ratio of current to square root of the potential rate. The departure of the three lines from a straight-line relationship at the higher rates of potential variation may be due in part to the larger iR drops occurring across the polarographic cell at these rates than at the lower rates. The magnitude of the iR drop invariably affects the linearity of the voltage sweep applied to the cell and hence the rate of the potential sweep at the dropping mercury electrode. Delahay (19) has studied, in a quantitative manner, the effect of a resistance in combination with the polarographic cell on the linearity of the potential sweep at a dropping mercury electrode. Increasing the total resistance decreases the linearity of the potential variation, and simultaneously decreases the peak current.

Another factor to consider in the relationship of i_p to $v^{1/2}$ is the rate at which zinc ion is reduced at the dropping mercury electrode. If the reaction at the

electrode proceeds at a moderate rate, the peak current will fall off at the higher rates of potential variation, which may well be the case for zinc ion as indicated by other experiments. The peak diffusion currents for the various zinc-ion concentrations were calculated by the present authors by equation 4 from Delahay's data and at a value of 5.75 for $v^{1/2}$. They are 258, 129, and 52 microamp., while the corresponding experimental values of Delahay are 56, 37, and 11 microamp. The percentage differences of the experimental values with respect to those calculated on a theoretical basis are 78, 71, and 80 per cent, respectively. This is a much greater deviation than the 28 per cent found by Randles (72) at a $v^{1/2}$ of 0.51 v. per second. The inability of the experimental values to conform to the theoretical equation indicates an irreversible electrode process for the reduction of zinc ion.

However, to test the validity of the oscillographic polarographic diffusion-current equation, only ions which are reduced reversibly at the mercury electrode should be used, since the diffusion-current equation is based on the hypothesis of reversible electrode reactions. Randles (72) has shown that the peak diffusion current for the reversible reduction of lead and thallium ions at the electrode agrees well with the theoretical values.

(b) Other factors

Other factors occurring in the theoretical equation derived by Randles and Sevcik have been experimentally tested. Both Sevcik (74) and Delahay (14) have shown the maximal peak current to be proportional to the concentration of the reducible species to a high degree of accuracy.

The variation of maximal peak current as a function of $t^{2/3}$ was studied by Delahay (14). An exact straight-line relationship was found for a 2.5×10^{-3} M manganous sulfate in 1 N potassium chloride solution. When $t = 0$, equation 4 predicts zero current. In the case of the manganous sulfate, when t equaled zero, the peak current was about 15 microamp. Here again theory is not in agreement with experiment, a result which indicates the need of an additive constant current factor in equation 4. Equation 9 predicts zero current when t equals zero. It is evident that another constant, which is independent of time, should be included in equation 9. Apparently when a mercury drop falls, a small amount of mercury is left at the tip and the current never actually drops to zero.

Equation 7 of Sevcik for the peak diffusion current may be written as

$$I_p = Km^{2/3}t^{2/3}v^{1/2}C \tag{10}$$

where K is a numerical constant depending on the nature of the reacting species and is given by the expression:

$$K = kn^{3/2}F^{3/2}D^{1/2} \tag{11}$$

In equation 11, k is a numerical constant. Delahay (14) calculated the values of K for zinc, chromate, and iodate ions from experimental data and found the values to be inconsistent with equation 11. Unfortunately, the reductive process for each of these three ions is probably irreversible. Sevcik (74), in his derivation

of equation 8, stated that it is supposed that the Nernst equation for the electrode potential holds at any instant up to a certain rate of change of potential; this is a tacit assumption that the reaction proceeds reversibly. Since the ions used are reduced irreversibly at the dropping mercury electrode, and therefore should not be used as a valid test of equation 11, the poor agreement between the values found from experimental data and from equation 11 can be expected. Equations 4 and 7, however, provide a means of testing the reversibility or irreversibility of an electrode reaction by comparison of the experimental peak-current values with those calculated from the theoretical equations. This procedure, in fact, has been explored by Delahay (16) and will be subsequently discussed.

Sevcik (74) has considered the current–potential curve for single and successive charging and discharging voltage-sweep cycles at an electrode of constant area. For the first cycle, only about 41 per cent of the anodic phase is oxidized, the rest being lost through diffusion. At the fiftieth cycle about 94 per cent of the amount reduced is converted by oxidation. The result of these changes is to incline and shift the zero-current line. After the fifteenth cycle, the charging and discharging curves are practically closed. It should be pointed out that, in practice, the two curves will never be completely closed at their extreme ends because of the unavoidable charging and discharging capacity currents present.

B. CAPACITY CURRENT

In addition to the peak-shaped diffusion currents, oscillographic polarography, as previously indicated, differs from classical polarography in another way. Because of the large differential capacity of the electrical double layer which exists at the mercury–solution interface, and the rapid rate of potential variation used in oscillographic work, a capacity current of comparatively large magnitude is produced.

The capacity current observed is due to a movement of electrons to or away from the electrode surface which movement is, accordingly, productive of current flow. This action is due to the charging of the electrode to the applied potential as the potential applied to the system is varied and is analogous to the charging of a condenser. The flow of current is therefore nonohmic and nonfaradaic in nature. The specific determination of movement of the electrons is indicated by the electrocapillary curve, with the net movement being zero at the electrocapillary maximum.

The general equation relating capacity (C) to charge (q) and potential (E) is:

$$q = CE \tag{12}$$

Differentiation of equation 12 with respect to time, t, leads to the expression

$$\frac{dq}{dt} = C\frac{dE}{dt} + E\frac{dC}{dt} \tag{13}$$

where (dq/dt) in coulombs per second is equal to the capacity current, i_c. Equation 13 may be rewritten in the form:

$$i_c = C\frac{dE}{dt} + E\frac{dC}{dt} \tag{14}$$

The capacity current as expressed by equation 14 may be broken up to correspond to two extreme cases: one, where the potential is constant or (dE/dt) is zero, and another, where the capacity is constant or (dC/dt) equals zero.

1. At constant potential

In considering the first case, we have the equation

$$i_{c_1} = E\frac{dC}{dt} \tag{15}$$

which holds for ordinary polarography at any instant during the life of a drop, and the capacity charging current is due to the increase in capacity of the electrical double layer as the area of the mercury drop increases with time. At the potential of the electrocapillary zero, where the charge of the electrical double layer is zero, the capacity current, i_{c_1}, is zero. As a result, equation 15 may be written as

$$i_{c_1} = (E_{max} - E_{de})\frac{dC}{dt} \tag{16}$$

where E_{max} is the potential of the electrocapillary maximum and E_{de} is the potential of the dropping electrode relative to some reference electrode. The value of (dC/dt) may be easily calculated by multiplying the capacity of the double layer by the rate of change of the area, A, of the drop, i.e.,

$$\frac{dC}{dt} = C\frac{dA}{dt} \tag{17}$$

Substituting equation 17 into 16, we have

$$i_{c_1} = (E_{max} - E_{de})C\frac{dA}{dt} \tag{18}$$

Evaluating the term (dA/dt) and substituting in equation 18 gives the capacity current as

$$i_{c_1} = 0.00564m^{2/3}t^{-1/3}C(E_{max} - E_{de}) \tag{19}$$

In equation 19, m is in milligrams per second, C is in microfarads per square centimeter, t is in seconds (starting from the time of the origin of the drop), $(E_{max} - E_{de})$ is in volts, and i_{c_1} is in microamperes. The value of C is dependent on the value of E_{de}. Usually, this value is lower at the more negative applied potentials and higher at the more positive applied potentials with respect to the potential of the electrocapillary maximum.

The numerical constant of equation 19 is smaller by a factor of 2/3 than that given by Kolthoff and Lingane (52, page 109). This 2/3 factor arises from the omission of the exponent factor of 2/3 for t in their differentiation of area with respect to time.

2. At constant capacity

Consideration of equation 14 with reference to the second case mentioned, i.e., for oscillographic conditions, results in the equation

$$i_{c_2} = C \frac{dE}{dt} \tag{20}$$

where (dE/dt) is the rate of potential variation in volts per second. The assumption is made that the differential capacity, C, as a function of potential is independent of the rate of potential variation at the mercury electrode. The time required for ionic equilibrium to take place in the electrical double layer is a microsecond or less (29). Since the rate of the applied voltage sweep is rarely less than 0.01 sec. per volt, the assumption is considered valid. When (dE/dt) is constant, the capacity current is proportional to the differential capacity of the double layer at any particular potential and any instant during the life of a drop.

TABLE 1

Values of capacity current calculated for three different conditions

CASE	m	t	i_{c_1}	$i_{c_{2A}}$	$i_{c_{2B}}$	$i_{c_{2A}}/i_{c_1}$	$i_{c_1}/i_{c_{2B}}$
	mg./sec.	*sec.*	*microamp.*	*microamp.*	*microamp.*		
I.....	2.0	4.0	0.11	6.8	0.0014	62	79
II.....	0.4	10.0	0.028	4.3	0.00086	150	33

To convert the capacity current of equation 20 into terms that will permit the calculation of i_{c_2} for any mercury drop at any time, we merely multiply the right-hand side by the area of the mercury surface to obtain

$$i_{c_2} = 0.00846 m^{2/3} t^{2/3} C \frac{dE}{dt} \tag{21}$$

where m, t, and C are in the same units as given for equation 19.

3. Justification for use of two separate equations

The reasons for separating equation 14 into two independent equations, one for ordinary polarography and the other for oscillographic polarography, may be made more evident by considering prototype cases. In table 1 are given values of capacity current calculated for three different conditions. The column headed i_{c_1} corresponds to the capacity current due to the changing area of the drop. Column $i_{c_{2A}}$ contains charging-current values under oscillographic conditions, while the column labeled $i_{c_{2B}}$ conforms to capacity-current values which would be obtained were the rate of potential change comparable to ordinary polarographic conditions. A differential capacity value of 20 microfarads per square centimeter was used in all of the example calculations. The value of $(E_{max} - E_{de})$ for equation 19 (column i_{c_1}) was chosen as 1.0 v. The currents, $i_{c_{2A}}$ and

$i_{c_{2B}}$, calculated from equation 21 correspond to (dE/dt) values of 10 and 0.002 v. per second, respectively.

Instead of limiting the comparison of the various charging currents to one set of m and t values, two sets were used which differ widely in their respective quantities. In one case (horizontal row I), m and t values simulate classical conditions. On the other hand, the second example (horizontal row II) corresponds to low m and high t values. Smith (75) has described capillaries capable of giving drop-times ranging from 16 sec. to 8 min.

Comparison of the various capacity-current values in table 1 may be found in the last two columns. When using the customary mercury drop-weight and drop-times (row I), the charging current under oscillographic methods ($i_{c_{2A}}$) is about 60 times greater than the capacity current, owing to the charging of the increasing area of the mercury drop. The contribution of the current in the latter case to the total capacity current is practically negligible. In the case of long drop-times and low drop-weights (row II), the ratio of the two currents ($i_{c_{2A}}/i_{c_1}$) increases to 150 and the contribution of i_{c_1} to the total current may be neglected. Hence, the capacity current for oscillographic work may be given by equation 21.

Of lesser importance is the ratio of i_{c_1} to $i_{c_{2B}}$ tabulated in the last column of table 1. Even though this ratio is decreased by employing longer drop-times, the currents obtained as a result of the 0.002 v. per second sweep are indeed so minute in both examples that present-day polarographs are not capable of detecting them. For classical conditions, then, the capacity current may be expressed by equation 19.

Delahay and Stiehl (19) have obtained a different relation by considering the capacity current obtained as a result of a linear voltage sweep applied to a dropping mercury electrode as

$$i_c = 4.81(m/d)^{2/3}t^{2/3}\left[E\frac{dC}{dE} + C\right]\frac{dE}{dt} + 3.20C(m/d)^{2/3}t^{-1/3}E \qquad (22)$$

where d is the density of mercury and the other terms are the same as previously designated. If the E terms of equation 22 are replaced by the quantity $(E_{max} - E_{de})$, then the second member on the right-hand side is identical with i_{c_1} of equation 19 and the first member on the right-hand side of equation 22 is the same as i_{c_2} of equation 21 except for the factor $E(dC/dE)$. Delahay and Stiehl included this factor to account for the fact that the capacity current varies with the potential, since (dC/dE) generally varies with E. However, it should be pointed out that in calculating differential capacity currents the values of C to be used are constantly changing, depending on the electrode potentials for which the capacity currents are calculated. Consequently, the capacity current varies with potential and should in fact be proportional to the differential capacity over the potential range covered. The use of appropriate values of C over the potential range considered in equation 22 should as a result preclude the need of the additional $E(dC/dE)$ term.

Loveland and Elving (59) have demonstrated that the capacity currents

obtained from a linear voltage sweep are proportional to the differential capacity of the electrical double layer at any potential of the dropping mercury electrode over the voltage span covered. The present authors have calculated the capacity currents for a 0.1 N potassium chloride solution as given by the first term of equation 22. It is found that the potential at which minimum current is indicated would come 0.05 v. more negative than that of the potential of minimum differential capacity (−0.28 v. *vs.* 0.1 N calomel electrode) and the potential of maximum current would be 0.08 v. more negative than the potential of maximum differential capacity (0.41 v. *vs.* 0.1 N calomel electrode). The potentials at which the maximum and minimum differential capacity currents are observed oscillographically (59) are practically identical with those of the potentials at which maximum and minimum capacity values occur, rather than those calculated from equation 22. It is, therefore, improbable that the capacity-current equation requires the extra term included by Delahay and Stiehl.

4. Differential capacity and surface charge density

Equation 21 may be arrived at from a different viewpoint. The equation relating differential capacity (C) to the surface charge density of the electrical double layer (Q) and the applied potential (E) is:

$$C = \frac{dQ}{dE} \tag{23}$$

Under oscillographic conditions, where a linearly increasing voltage sweep is applied to the dropping mercury electrode, the rate of change of potential with respect to time, t, is equal to a constant, K:

$$\frac{dE}{dt} = K \tag{24}$$

Substituting the value of dE of equation 24 into equation 23, we have:

$$C = \frac{1}{K}\frac{dQ}{dt} \tag{25}$$

or

$$\frac{dQ}{dt} = KC = C\frac{dE}{dt} = i_{c_2} \tag{26}$$

Equation 26 is identical in form with equation 20, where the rate of flow of charge (dQ/dt) is equal to the capacity current, i_{c_2}, which is proportional to the differential capacity of the electrical double layer. The same assumption concerning the independency of the differential capacity with the rate of voltage variation is made here as in the case of equation 20.

If equation 20 or 26 is satisfied experimentally and the contribution of the capacity current due to the charging of a growing mercury drop can be ignored (which it can with long drop-times), the i–E relationship observed should be

identical with the shape of a curve of differential capacity as a function of potential difference. That this is the case will be discussed subsequently.

Integration of equation 23 leads to an equation for the surface charge density:

$$Q = -\int_{E_{max}}^{E_{de}} C \, dE \tag{27}$$

where Q is the surface charge in microcoulombs per square centimeter, C is the differential capacity in microfarads per square centimeter, and E_{de} and E_{max} have the same meanings as mentioned previously. The limits are taken with reference to E_{max}, since Q is zero at the potential of the electrocapillary maximum.

The values of Q can be obtained by graphical integration (30) of known capacity values. By electronic integration of the differential capacity–potential relation, oscillograms for surface charge density may be observed in a few seconds or less (60).

Further integration of equation 27 leads to an expression of surface tension *vs.* potential or the so-called electrocapillary curve. By performing a double electronic integration of the differential capacity–potential relation, it is possible to observe the electrocapillary curve (60).

IV. Experimental Circuits

A. Current–potential patterns

The first application of the cathode-ray oscilloscope to the measurement of polarographic phenomena was reported by Matheson and Nichols (61) in 1938. The original apparatus employed a 60-cycle sine-wave voltage of 1.5 v. peak to polarize the polarographic cell. A direct-voltage bias was supplied to the alternating voltage so that the potential at the cell varied sinusoidally from about 0 to −3 v. with respect to the calomel reference electrode. The A.C. voltage applied to the cell also furnished the signal for controlling the horizontal deflection of the oscilloscope. A resistance in series with the cell provided a voltage drop proportional to the current passing through the cell. This voltage drop was amplified to control the vertical deflection of the oscilloscope. The resulting oscillogram was an i–E pattern occurring 60 times each second. Reproducible traces were obtained by synchronizing the mercury drops with the frequency of the applied voltage, i.e., 60 drops per second. The practicability of using such short drop-times is questionable from the viewpoint of stirring effects.

The application of a linear voltage sweep was also reported by the same investigators. Figure 3 is a schematic diagram of their apparatus. The periodic charging of a capacitor C through a variable resistor R_2 of 30K ohms gives a linear voltage sweep (30 cycles per second, 0 to −2.4 v.) to the dropping mercury electrode. Sweep renewal is obtained by shorting capacitor C for an instant by contact K. The resulting current is measured by placing a known resistance, R_1, in series with the cell; the iR_1 drop is applied to the vertical deflection plates after suitable amplification. When R_1 is large (100K ohms), no peaks occur in the i–E oscillogram, since (di/dt) becomes constant and a major portion of the

total voltage drop is across R_1; when R_1 is small (60 ohms), the curves are quite peaked (figure 4). By using a capillary of inner diameter between 0.035 and 0.060 mm., Matheson and Nichols were able to synchronize the drops of mercury with the 20- and 60-cycle sweeps by adjusting the head of mercury and the maximum voltage across the cell.

1. Saw-tooth sweep

The oscillographic technique of obtaining *i–E* curves then lay dormant for about ten years until Randles (70, 72) reported his investigations in this field.

When a steadily changing voltage difference is applied to a polarographic cell and a resistance in series, the rate of change of potential with respect to time, (dE/dt), at the dropping mercury electrode is affected by the voltage drop across the resistance. Randles (72) has developed a circuit which avoids this effect 99 per cent efficiently by the use of a cathode follower circuit with feedback. The instrument is quite complex and a complete description of it is be-

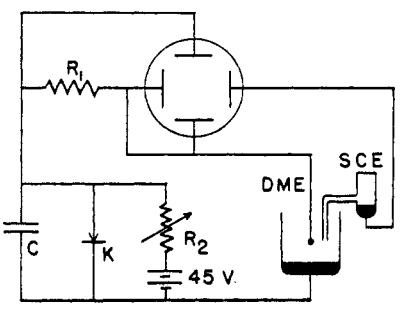

FIG. 3.

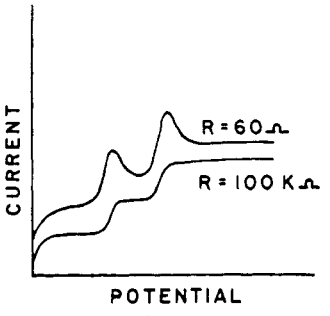

FIG. 4.

FIG. 3. Circuit of Matheson and Nichols (61) for producing a linear voltage sweep to the polarographic cell.

FIG. 4. Effect of series resistance on the shape of the current–potential relation

yond the scope of this review. Some of the more important features of the arrangement, however, may be mentioned. The current-indicating resistor could be varied from 2K to 94K ohms in seventy-nine steps. Voltage sweeps were developed by the charging of an 8-microfarad electrolytic capacitor through resistances ranging from 0.5 to 5.0 megohms in eight steps to give eight different voltage-sweep frequencies. This provided voltage variations ranging from 0.14 to 0.88 v. per second. The starting potential of the sweep is controlled by a biasing circuit. Because the voltage changes involved are slow, direct coupled amplifiers were used for horizontal and vertical amplification.

In order to reproduce current peak heights, the voltage sweep was always applied at the same age of the mercury drop, preferably during the last few seconds of the drop-life, since the rate of change of the area of the drop is least at the end of the drop-life. The sudden decrease in current which occurred across the series current-measuring resistance when the mercury drop fell was used to activate a flip-flop circuit which in turn energized a relay. Once energized,

the relay closed a contact, shorting the charging capacitor used for providing the potential sweep. Current continued to flow through the relay for a length of time depending on the resistance and capacity values in the flip-flop circuit. At the end of that time the relay was deënergized, the contact opened, and the voltage sweep to the cell initiated. The sweep ended when the mercury drop fell and the cycle repeated.

The system silver/silver chloride reference electrode *vs.* the dropping mercury electrode was used for all solutions. The solution resistance was less than 100 ohms in 1 *M* potassium chloride solution when the two electrodes were 0.25 in. apart.

More recently, Delahay (14) has described a circuit for obtaining *i–E* oscillograms in which a saw-tooth voltage is taken from the cathode resistor of a cathode follower circuit and applied to the polarographic cell. The horizontal deflection of the cathode-ray oscilloscope is proportional to the voltage applied to the cell and the vertical deflection is proportional to the current flowing through the cell. The starting potential of the voltage sweep is controlled by a biasing potentiometer circuit. Photographs of the oscillograms are made for a duration corresponding to the life of a few mercury drops at the electrode. Only the highest wave, corresponding to the maximal area of the drop, is taken into consideration.

In this type of instrument, the voltage sweep starts almost at the same instant as the preceding one ends. As a result, oxidation of the substance which is reduced on one sweep occurs when the next sweep starts; this gives rise to both capacity and anodic currents flowing at the early part of the oscillographic wave. To eliminate the anodic portion as much as possible, Delahay (15) developed a circuit which produces a quiescent period before each applied voltage sweep, during which time almost all of the reduced material is oxidized. The main part of this circuit consists of a duo-diode which effectively clips a portion of a saw-tooth wave to a constant voltage before the signal is applied to the cell. The constant-voltage portion of the sweep corresponds to the quiescent period.

One of the latest circuits for producing *i–E* traces on the cathode-ray oscilloscope has been described by Snowden and Page (76). The individual units composing the instrument are discussed in detail in their paper. The main features of the apparatus are: (*1*) a delay gate for synchronizing the linear voltage sweep across the mercury cell with the drops of mercury, (*2*) a voltage clipper to prevent excess sweep voltages from being applied to the cell, and (*3*) a compensator to maintain the potential at the dropping mercury electrode independent of the voltage drop across the resistor in series with it. Such compensating circuits are of advantage only when the voltage drop across the series resistor is greater than or of the same order of magnitude as the voltage drop across the solution. If the vertical amplification is sufficiently large to give oscilloscope sensitivities of 0.001 v. or less input per inch vertical deflection, the linearity of the voltage sweep will be little affected by this small *iR* drop across the series resistor. In fact, at such high vertical amplification the solution resistance is usually greater than the current-measuring resistance and, in

such cases, the iR drop across the solution resistance may become the more dominating factor affecting the linearity of the cell potential. To the knowledge of the present authors there is no direct means of compensation for the voltage drop across the solution, as there is for the voltage drop across the series resistor.

The delay gate of Snowden and Page functions in a manner similar to that described by Randles. The voltage sweeps are delayed until the last 0.1 to 0.5 sec. to the drop-time. The circuit has the additional feature, however, that it blanks the oscilloscope during the delay time, and the trace is visible only during the length of time the sweep is operating.

2. *Triangular sweep*

An innovation in the technique of oscillographic i–E curves was introduced by Sevcik (74). The current–potential patterns are produced by a periodic equilateral triangular voltage sweep, charging and discharging the dropping mercury electrode linearly with time. Each complete cycle gives one cathodic and one anodic branch, the comparison of which serves to indicate the reversi-

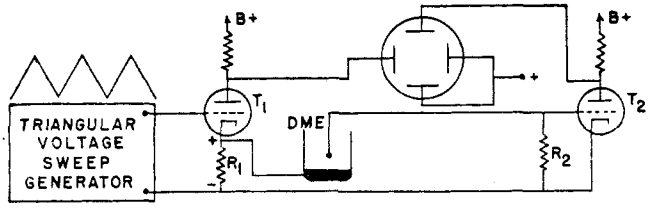

FIG. 5. Schematic diagram of Sevcik's apparatus (74) utilizing a triangular voltage sweep.

bility of the electrode processes. The arrangement (figure 5) consists of a periodic triangular sweep generator, the output of which is placed on the grid of tube T_1. The cathode voltage developed across resistance R_1 varies in accordance with the variation of the grid voltage. The positive portion of the voltage developed at the cathode of the tube leads to the unpolarized reference electrode, a pool of mercury. The polarized electrode is connected to the negative side by means of the resistance R_2 (0 to 10K ohms). The iR_2 drop is proportional to the current passed by the cell and is applied to the grid of tube T_2, amplified, and used to give the vertical deflection on the cathode-ray oscilloscope. The voltage at the plate of tube T_1 varies in the same manner as the voltage applied to the cell and is used for horizontal deflection, an exact linearity between potential and deflection being expected. This is not exactly true, since the iR_2 drop which is in series with the cell as well as the voltage drop across the solution resistance causes the linearity of the cell potential to deviate slightly, depending on the amount of current passing through the cell. Sweep frequencies of 0.795, 3.55, 20.8, and 73.4 cycles per second were used. The influence of the growth of the drop on the current was eliminated by registering the i–E curve immedi-

ately before the drop fell. Such an arrangement has the advantage of eliminating the use of a shorting contact for sweep renewals as employed in the previous circuits described.

Loveland and Elving (59) have investigated the applicability of a circuit similar to that used by Sevcik (74) and by Bieber and Trumpler (4) for studying polarographic phenomena. Essentially, a square wave is integrated to give a triangular voltage signal which is amplified by a power tetrode tube. The triangular voltage wave applied to the cell is supplied from the cathode resistor of the tetrode. The remaining portion of the circuit (current-measuring resistance and amplifier) is of conventional design.

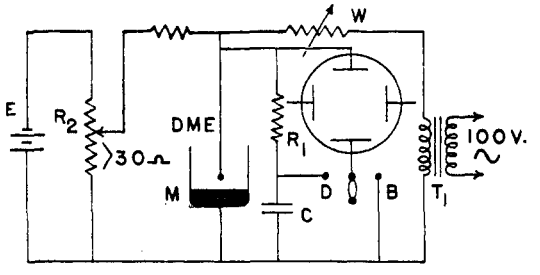

FIG. 6.

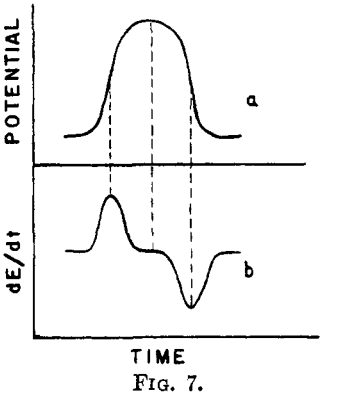

FIG. 7.

FIG. 6. Heyrovsky's circuit (41) for producing potential–time and derivative oscillograms.

FIG. 7. Potential–time and derivative curves of a nonelectroactive (reducible or oxidizable) electrolyte solution.

B. POTENTIAL–TIME AND DERIVATIVE PATTERNS

A different approach to oscillographic observation of polarized electrodes was made by Heyrovsky and Forejt (34, 36, 37, 39, 40, 41, 42, 46, 47). Their circuit (figure 6) is used to produce either the potential–time relationship or the first derivative of the potential–time curve. A 100-v., 50-c.p.s., sine-wave or square-wave voltage is applied by means of the transformer T_1 to the polarographic cell M through a variable resistor W of from 0.3 to 2 megohms. The resistance W is made very large to insure constant current impulses regardless of any changes in the back E.M.F. of the cell. A direct current from the variable resistance R_2 and battery E is superimposed on the alternating current so that the cell potential will be within the limits of about 0 to 2 v. *vs.* the standard calomel electrode. To produce a stationary potential–time pattern on the screen, the voltage across the cell is applied, after amplification to the vertical deflection plates of the oscilloscope (switch set at point B) and the frequency of the time sweep is synchronized to that of the applied alternating voltage. When the frequency of the time base is increased to about 100,000 cycles per second, the kinks of the potential–time curve are extended to lines, providing an oscillo-

graphic spectrum (35, page 237; 44, 46). The only notable advantage of this innovation is that the E–t curves are suitable for a quick qualitative analysis.

When the switch is placed on point D, the differential of the potential–time curve is obtained on the oscilloscope. In this position the vertical deflection is proportional to the iR drop across the resistance R_1. The current which passes through R_1 must also pass through capacitor C, and, since the current which passes through the capacitor is a function of the rate of change of potential, the vertical deflection actually gives the derivative, (dE/dt). When the sweep frequency of the horizontal deflection is synchronized with that of the applied voltage, a pattern is obtained which represents (dE/dt) *vs.* time. To avoid the complication of the periodically changing area of the dropping mercury electrode, a streaming mercury electrode was introduced which has the advantage of maintaining a constant electrode area in contact with the solution, thus giving steady oscillograms (38).

A typical potential–time trace obtained for a base solution without any depolarizer is illustrated in figure 7a; the differential of this curve is shown in b. The left branches of the two curves correspond to cathodic polarization and the right branches to anodic polarization. Where the slope of the E *vs.* t curve is greatest, a maximum occurs in the (dE/dt) *vs.* t curve; where the slope of the curve is a minimum or, in this case, zero, (dE/dt) has the value of zero, which corresponds to the middle flat portion of the differential curve. Whenever a depolarizing reaction or a change of capacity takes place at the mercury electrode, a current flows at the electrode. This current flow produces a time-lag or horizontal deflection in the potential–time pattern (in figure 16).

The first use of the triangular voltage sweep in oscillographic polarography was reported by Bieber and Trumpler (4). Whereas Sevcik used this type of voltage sweep to study current–potential relationships, Bieber and Trumpler used the triangular sweep for investigating potential–time characteristics. The triangular-shaped wave was produced by electronic integration of the square-wave signal produced by a multivibrator circuit. The triangular wave was amplified and the output appearing across the cathode resistor of the amplifier was used to charge and discharge either a dropping mercury electrode or a streaming mercury electrode. The rapidly changing voltage across the cell was used to deflect the oscillographic trace vertically. The frequency of the horizontal sweep was synchronized with that of the triangular sweep to give steady potential–time patterns. These patterns are similar in all respects to those obtained with Heyrovsky's circuit, where time-lags occur when depolarization processes take place.

Bernheim and Fournier (3) polarographically studied solutions of sodium zincate by superimposing an alternating potential of 1 v. on a direct potential of 1 v., thus obtaining a potential change of 0–2 v. at the mercury electrode. The change in potential was studied as a function of time by means of a cathode-ray oscilloscope.

Fournier and Quintin (23) have investigated some of the characteristics of potential–time oscillograms for a number of reducible ions. They found that

the potential of the steps of the E–t patterns was independent of the frequency of the applied alternating voltage, whereas the width of the steps decreased as the inverse of the square root of the frequency up to a certain limiting frequency. This frequency limit depended on the nature of the ion and on the base solution used.

C. CURRENT–TIME PATTERNS

The study of polarographic current as a function of the time during which a mercury drop grows has been investigated with the aid of a cathode-ray oscilloscope by Bon and Reboul (8, 9). They used the simplest of polarographic circuits, consisting of a battery, a polarographic cell, and a current-measuring resistance. The vertical input of the oscilloscope was connected across the current-measuring resistance so that the vertical deflection of the oscillographic trace indicated the current flowing through the cell at any instant. The horizontal deflection of the trace was proportional to the time during the life of a mercury drop and the pattern obtained had a current–time relationship. A typical current–time oscillogram for a single mercury drop for a diffusion-controlled process is shown in figure 8.

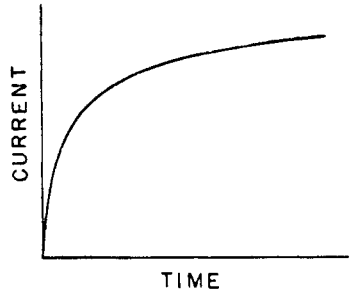

FIG. 8. Current–time relationship for a diffusion-controlled process

Taylor *et al.* (78) recorded current–time oscillograms in a manner which required that the polarographic current signal be amplified and applied directly to the vertical deflection plates of the cathode-ray oscilloscope. The vertical deflection of the oscilloscope beam was then photographically recorded on a drum camera, which revolved at a known peripheral speed and thus provided a time axis. With drop-times of about 3.5 sec. for the dropping mercury electrode it was possible to record the instantaneous current values for seven or eight successive mercury drops. Others (2, 5, 10, 33, 40, 51, 79, 80) have reported the use of oscillographic current–time techniques to the observation of polarographic phenomena which will be discussed subsequently.

D. DETERMINATION OF HALF-WAVE POTENTIALS

The direct determination of half-wave potentials has been reported by Müller, Garman, Droz, and Petras (64). Their principle of operation is elucidated in figures 9 and 10. An E.M.F., V, is taken off resistance R_2 and applied to the

dropping mercury electrode. A small alternating voltage, Δv, taken from resistance R_3, varies about point H to give wave S. The amplitude of S depends on the steepness of the linear portion of the polarographic curve AHB. If V shifts, then S becomes distorted because of intersection with the nonlinear portion at A or B. When the applied direct voltage is adjusted to the half-wave potential H, a perfectly symmetrical sinusoidal figure S appears on the cathode-ray oscilloscope. The alternating current which passes through the cell is amplified about 4×10^3 times and applied to the vertical deflection plates of the oscil-

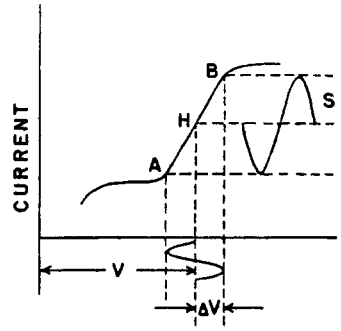

FIG. 9.

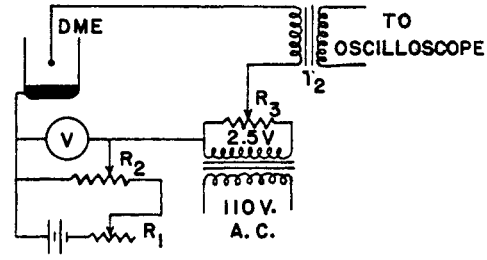

FIG. 10.

FIG. 9. Determination of the half-wave potential oscillographically
FIG. 10. Circuit used by Müller *et al.* (64) for determining half-wave potentials

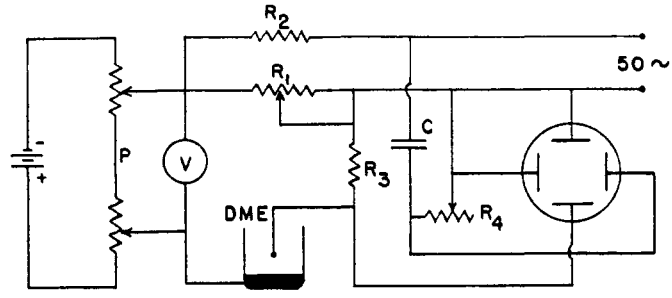

FIG. 11. Circuit used by Boeke and van Suchtelen (7) for determining half-wave potentials.

loscope.[1] The sweep frequency of the oscilloscope is synchronized with the 60-cycle applied alternating current to produce the sine-wave pattern.

The pattern disappears as each mercury drop falls from the capillary. A new curve appears immediately and the interruption does not disturb the results. Observed half-wave potentials are reproducible, varying by only a few millivolts.

Essentially, the same principle of observing half-wave potentials was used by Boeke and van Suchtelen (6, 7). However, in their circuit (figure 11) the internal sweep of the cathode-ray oscilloscope is replaced by the 50-c.p.s. A.C. voltage through condenser C and resistance R_4. The voltage drop across the series cur-

rent-measuring resistance, R_3, is amplified and used for the vertical deflection of the oscilloscope trace. The direct voltage is applied to the polarographic cell by potentiometer P. When the small A.C. voltage varies about the linear portion of the diffusion current wave, i.e., about the half-wave potential, the A.C. signal is reproduced across R_3; the vertical and horizontal alternating waveforms are in phase and a straight line is observed on the screen of the oscilloscope. When the applied voltage is increased or decreased from the half-wave potential value, the small A.C. voltage intersects the nonlinear portions of the diffusion wave, and the sinusoidal waveform of the current through R_3 is deformed. The resulting pattern loses part of its linearity and becomes loop-shaped at either end, depending on whether the applied direct voltage is greater or less than the half-wave potential.

Boeke and van Suchtelen (7) have described another circuit for determining half-wave potentials in which the polarographic cell forms one arm of an alternating-current bridge. A small alternating voltage is impressed across the bridge, which passes through a potentiometer supplying direct voltage for the bridge. The bridge is brought to equilibrium as indicated by a reduction to minimum area of a luminous cross, observed on an electron-ray tuning indicator. The complete potential scale is run through and the potentials at which maximum luminous areas on the tuning indicator occur are read. At these particular points, the half-wave potentials of the reducible species occur and the bridge requires balancing again. The amount of balancing required is a measure of the concentration of the ion reduced at that potential. Thus the instrument can discriminate between reducible ions both qualitatively and quantitatively.

Brief discussions of these and some of the other types of oscillographic polarographic instruments mentioned have been given by Jones (49, 50) and more recently by Lingane (56, 57).

V. Applications and Results

A. ANALYSIS

1. Qualitative

Qualitative measurements of half-wave potentials obtained by the oscillographic methods of Müller *et al.* (64) and Boeke and van Suchtelen (7) are comparable in accuracy to those of ordinary polarography. For example, Müller *et al.* observed the half-wave potential for cadmium to be 0.627 to 0.629 v. *vs.* the saturated calomel electrode, a result which is in fair agreement with other polarographic data. The half-wave potentials are reproduced with high precision. Snowden and Page (76) differentiated the current–potential pattern prior to presentation on the face of the oscilloscope to obtain pips in place of the usual peak curents. The potentials at which the pips occur can be used in a qualitative scheme. The method of Boeke and van Suchtelen (7) was extensively employed by Prytz and Osterud (68) for determining the influence of certain electrolytes and suppressors on the half-wave potentials of several metal ions.

In another technique involving (dE/dt)–E oscillograms obtained with a stream-

ing mercury electrode, Heyrovsky (44, 45) was able to differentiate between *o*-, *m*-, and *p*-nitrophenols even in the presence of nitrobenzene. By the same method, the isomeric acids nicotinic, picolinic, and isonicotinic were distinguishable in 2 *N* sulfuric acid. With the dropping mercury electrode, the oscillograms became complicated, owing to simultaneous side-reactions occurring at the electrode surface.

2. Quantitative

(a) Peak-height measurement

According to equation 4 or 7, the maximum peak diffusion current is proportional to the concentration of the reducible species. Although these equations were deduced for reversible electrode processes, the proportionality between the maximum peak current and concentration has been experimentally verified by several investigators (14, 72, 74) for both reversible and irreversible reductions. Matheson and Nichols (61) were the first to point out the analytical possibilities of the oscillographic technique to both inorganic and organic systems. It was left to Randles (72), however, to devise and demonstrate an accurate quantitative procedure. Instead of measuring the peak height of the diffusion current, the current-measuring resistance is varied until the peak height corresponds to a standard height. The value of the current-measuring resistance is inversely proportional to the peak current. The primary advantage of this method is the elimination of any errors due to nonlinearity of amplification. For calibration purposes, standard solutions can be used and the peak height brought to the standard height.

An alternative procedure of quantitative analysis involves measuring peak heights for a definite setting of the current-measuring resistance. The main disadvantage of this method is in the difficulty of accurately measuring the peak height. Moreover, amplification of the various peak heights may not be linear over the ranges covered. Snowden and Page (76) have experimented with both methods of quantitative measurement and report that the former method is accurate within ± 2 per cent while the latter method is accurate to only about ± 4 per cent. Where the concentration of the reducible ions was very small, the width of the trace on the cathode-ray oscilloscope became a limiting factor.

The additive technique of calibration may be used, whereby the peak height of the unknown sample is adjusted to the standard height and then a known amount of the solution is added and the measurement repeated. In still another calibration method, a "pilot" ion may be added to the solution to be tested and the peak current adjusted to the standard height for each ion present.

When voltage-sweep rates are about 5 v. per second or greater, the capacity current becomes noticeable and the maximal peak current is determined in two ways depending on the circumstances involved (14). If the height of the wave is very great in comparison with the capacity current, it is sufficient to measure the height from the tip of the peak to a line drawn tangent to the horizontal portion of the curve just before the wave begins (figure 12A). If, however, the concentration is small and the maximal peak current is smaller than the capac-

ity current, a distortion of the wave occurs and a different method must be used to find the maximum current (figure 12B). The capacity current is extrapolated by continuation of the capacity-current curve. The peak-current height is then the height from the peak of the cuve to the extrapolated capacity-current line (figure 12B). The application of this technique for determining peak currents has been illustrated in full by Delahay (14). An oscillogram of the pure base solution when superimposed on the oscillogram of diffusion current of the ion reduced would indicate more accurately the base line to be taken for calculation of the peak height.

(b) Other types

The quantitative measurement of concentration by oscillographic means is not limited to the use of current–potential oscillograms. A procedure was developed by Heyrovsky and Forejt (46) whereby the derivative of the potential–time curve is used to indicate the concentration of a reducible species. Where a

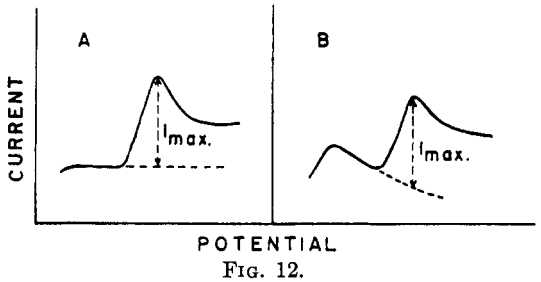

FIG. 12.

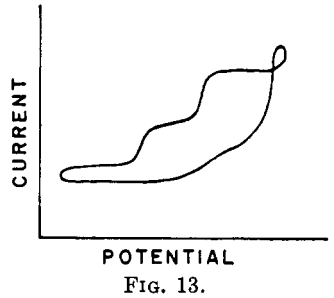

FIG. 13.

FIG. 12. Measurement of peak-current heights: (A) with negligible capacity current; (B) with appreciable capacity current.

FIG. 13. Current–potential relationship for 1 mM manganous chloride and 2 mM aluminum chloride in 0.1 N lithium chloride.

time-lag occurs in the potential–time curve owing to the reduction or oxidation of a chemical species, a v-shaped notch appears in the differential of the potential–time pattern. The depth of the notch is a nonlinear function of the concentration of the ion in solution. An empirical calibration curve must be made in order to measure concentrations. The method is not as accurate as that of the current–potential technique and therefore is seldom used.

Heyrovsky (44) has worked out an oscillographic differential method of quantitative analysis which is capable of determining concentrations of depolarizers of the order of 5×10^{-7} to 10^{-6} M. The arrangement uses the triangular voltage sweep circuit of Sevcik (74) and twin dropping electrodes so that charging currents and oxygen waves are compensated.

Airey (1) has compared the cathode-ray oscilloscope with photographic and pen-recording polarographs, and found the oscilloscope to be superior in sensitivity and in speed, about the same in accuracy, and inferior as far as complexity and size are concerned.

By integrating the peak currents obtained in current–potential oscillograms, Snowden and Page (76) were able to produce a curve which contained S-shaped steps similar to those obtained in ordinary polarographic procedure. The information obtainable from such an oscillogram, however, is no greater than that from the *i–E* curve prior to integration.

3. Separation of waves

Of analytical importance is the influence of prior reductions on the peak diffusion-current height of the ion of which the concentration is to be measured. Randles (72) has found that, provided the potential sweep is started at a potential at which all earlier reductions are occurring, the peak height of the ion under measurement is not altered appreciably. A minimum of 0.2 v. difference between the half-wave potential of the ion of which the concentration is being determined and that of any of the other ions present is required to accomplish the desired quantitative measurement without excessive error. This is approximately the same difference in half-wave potentials as is required in ordinary polarography to separate diffusion-current waves of two reducible ions. Airey (1) has stated that it is possible to estimate cadmium in amounts fifty times or more greater than lead by starting the potential sweep at −0.5 v. *vs.* the standard calomel electrode. The half-wave potentials of lead and cadmium are −0.4 and −0.6 v., respectively, *vs.* the standard calomel electrode.

On the other hand, Snowden and Page (76) report that if the half-wave potentials of two ions are separated by at least 0.25 v., accurate quantitative measurements can be performed on no more than a fivefold difference in concentration. The inability of the circuit of Snowden and Page to analyze greater differences in concentrations as compared to the apparatus of Randles is probably due to the faster rate of voltage change used. Since Snowden and Page used voltage sweeps of 1- to 2-sec. duration, the potential variation in their case is about five times as great as that employed by Randles. The faster the potential sweep, the less time is available for the limiting diffusion current to be reached. This results in the peak diffusion current of the more difficultly reducible ion superimposing its value on the diffusion current of the more easily reducible ion at a higher current value of the latter than it would at a lower rate of potential sweep. In other words, the lower the rate of potential variation, the better the separation between diffusion currents for a given difference in the half-wave potentials of two reducible species. The higher rates of potential change which Snowden and Page used explain the smaller differences in concentration which they can determine in comparison to those which Randles is able to measure.

Breyer *et al.* (12, 13) have developed a method of polarography employing alternating currents. Although the current-indicating device does not employ a cathode-ray oscilloscope, none the less the method is novel and worth mentioning. A small sinusoidal voltage of 1–90 mv. is superposed on a direct voltage applied to the polarographic cell. The alternating current flowing through the cell at a given applied voltage is amplified and the resultant current read by

means of a vacuum-tube voltmeter arrangement. At the half-wave potential of a reducible species the alternating current is at a maximum. The magnitude of the maximum current is an indication of the concentration of the reacting species. A plot of potential *vs.* alternating current gives rise to peak curves instead of the S-shaped curves of ordinary polarography. The technique has the distinct advantage of separating polarographic waves only 40 mv. apart. However, the latter would apparently be true only if the waves had slopes approximating to polarographic n values of 1 or greater.

B. ELECTRODE KINETICS AND REVERSIBILITY

Oscillographic polarography is much better adapted to the study of the degree of reversibility or irreversibility of electrode reactions than are the conventional methods of polarography. Heyrovsky (37, 42) defines the term "oscillographic irreversibility" as meaning that the anodic and cathodic processes are different, but implies that each of the processes may by itself be reversible. The present authors prefer to view the question of irreversibility from three points of view: (*1*) the anodic and cathodic processes occur fairly rapidly at different half-wave potentials, implying different electrode mechanisms for the two processes; (*2*) the anodic and cathodic processes occur at the same potential but the rates of the reduction or oxidation processes or of both are slow, diffusion is of minor importance, and hence the limiting current is determined by the kinetics of the electrode reaction; and (*3*) a combination of the two preceding situations. Examples of the first two conditions are prevalent in the literature. By the term "reversible" we mean that the oxidation and reduction half-wave potentials are identical and that the two processes are so rapid that the currents are governed by diffusion.

The irreversibility of electrode processes demonstrates itself in oscillographic work in many ways. The most obvious feature in current–potential oscillograms for irreversible reductions is the rounding off of the peak current, which in some instances manifests itself by a mere change in the slope of the curve. Where both charging and discharging potential sweeps are used, oxidation and reduction half-wave potentials may be compared to give information concerning the reversibility of the electrode process. The symmetry of kinks on the two branches of the potential–time curves can be used in the same manner. The deviation of the maximal peak current from the value calculated from the theoretical equation as a function of the square root of the potential variation is indicative of the degree of reversibility or irreversibility of the electrode reaction. Another procedure involves the dependency of the maximal peak current on the pressure head of mercury; for a reversible system maximal peak current is theoretically independent of the pressure head of the mercury.

1. Current–potential patterns

Matheson and Nichols (61) were the first to obtain an i–E oscillographic curve of an irreversible reaction, although the explanation of the shape of the curve did not involve consideration of this aspect. A solution of 1 millimolar man-

ganous chloride and 2 millimolar aluminum chloride in 0.1 *N* lithium chloride was used (figure 13). The lower or oxidation trace shows little or no current change in comparison to the upper or reduction curve. The authors explain this as being due to the partial exhaustion of reducible material near the interface of the electrode, owing to currents drawn at voltages higher than the reduction potential. The appearance of a reduction curve but no oxidation curve is likewise explicable on the basis that manganous and aluminum ions are reduced but not readily oxidized at the mercury electrode under rapidly changing applied voltages. Heyrovsky (42) observed this to be the case when using the potential–time technique on manganous ion in neutral or ammoniacal solution.

(a) Shape of peak current

A rather thorough investigation of the current–potential characteristics of reducible ions was made by Randles (72). Unsatisfactory results were obtained when a stationary platinum microelectrode was used. With the platinum electrode an interval of 7–10 sec. must be allowed for the reduced metal to return

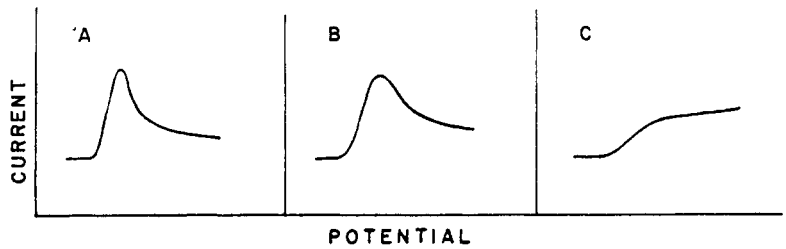

FIG. 14. Shape of current–potential oscillograms obtained with a linear voltage sweep for: (A) the reversible reaction involving lead ion, (B) the slightly irreversible reaction involving zinc ion, and (C) the irreversible reaction involving nickel ion.

to solution and the concentration to regain its original status. Reduction occurs at more negative potentials and the wave is less peaked with the platinum electrode than with the dropping mercury electrode. All quantitative measurements were carried out with the latter electrode.

Several metal ions were investigated, whose redox behavior was classified by Randles according to the observed polarograms as reversible, irreversible, or diverging from reversibility. The reversible reactions are characterized by their very sharp peak current, as in the case of cadmium ion in 1 *M* potassium chloride (figure 14A). A divergence from reversibility is manifested by a rounding off of the peak-current curve, as in the case of zinc ion in 1 *M* potassium chloride (figure 14B). The irreversible reaction is exemplified by a very rounded current peak or in some cases by a flat wave, as in the case of nickel ion in 1 *M* potassium chloride (figure 14C). The effect of adding a reagent for hastening the electrode process is easily followed. Thus, the addition of potassium thiocyanate to the nickel solution of figure 14C transforms the flat wave into a well-defined peaked wave similar to figure 14A. Cobalt behaves much the same as nickel. For reversible reactions, the width of the current peak is inversely proportional to

n, the number of electrons transferred per ion reduced. Thus, the oscillogram for the reduction of bismuth is more peaked than that for cadmium, which in turn is more peaked than that in the case of thallium.

Oscillographic current–potential curves may be used on organic systems as well as inorganic. An i–E oscillogram obtained by Sevcik (74) for phenylglyoxylic acid at a pH of 8 showed a cathodic peak current without any anodic current, indicating the irreversibility of the reduction.

(b) Height of peak current

Delahay (16) has compared the equations for maximal peak current developed by Randles (equation 4) and Sevcik (equation 7) and indicated their identity except for the numerical constant. The experimental results obtained by Delahay for the peak current in reversible reactions corresponded closely to calculations based on Randles' equation, and less accurately on Sevcik's equation. For irreversible reactions neither equation seemed to fit the data.

(*i*) *Dependency on the rate of potential change:* The variation of maximal peak current with the rate of potential change was studied by Delahay (16) with several ions (hydrogen, thallous, cadmium, lead, nickel, antimony, and iodate) in various supporting electrolytes and the results were compared with the values calculated from Randles' equation. The shape of the curve (maximal peak current *vs.* square root of the rate of potential change) was used as a criterion of reversibility, since the extent of the departure of the experimental curve from the theoretically calculated straight line indicates the degree of irreversibility of the electrode process. Of the seven reducible ions studied, only the data for thallous ion agreed closely with the values predicted from Randles' equation. Lead and cadmium gave slightly curved lines, the negative deviation of the peak current from the theoretical values increasing with increasing rate of potential sweep; thus, cadmium and lead are to be considered slightly irreversible. The other ions studied showed much greater deviations, especially nickel ion in tetramethylammonium bromide and iodate ion in sodium hydroxide.

The curves are interpreted by assuming that for irreversible reactions the rate of electrode reaction is a factor controlling the height of the peak current. As the rate of potential variation increases, the influence of the electrode reaction rate becomes more pronounced. For a reversible electrode no rate effect should be observed and Randles' equation should be applicable, as in the case of the reduction of thallous ion. For an irreversible electrode reaction the rate effect will depend on the free energy of activation of the process involved. The greater the free energy of activation for a given process, the more irreversible that process is.

In a more recent paper, Delahay and Perkins (17) have discussed phenomena occurring during the quiescent period of a voltage sweep. Their data indicate that for irreversible reactions the curvature of the graph of i_p *vs.* $v^{1/2}$ is accountable not only on the basis of the rate of the cathodic process but also on a decrease in the concentration of reducible material before each applied voltage sweep as the mercury drop grows.

Under the conditions of Delahay's experiment the higher the peak current, the greater the effect of the solution resistance becomes (assuming the iR drop across the current-measuring resistance to be negligible). This effect invariably will decrease the rate of potential variation more at the higher than at the lower sweep rates. As a result, the height of the maximal peak current decreases with increasing rates of potential variation as observed for the slightly irreversible reactions. However, the magnitude of this effect is probably not sufficient to invalidate the results.

The variation of wave height with rate of potential change was further investigated by Delahay and Perkins (18) by comparing the wave heights for the reduction of hydrogen, cobaltous, and iodate ions under two different conditions of voltage sweep. In one case, only a single voltage sweep was used, while in the other case a repeating voltage sweep was applied to the dropping mercury electrode. Higher peak currents ensued when single sweeps were employed. This difference was ascribed to a decrease in concentration of reducible substance at the surface of the mercury drop caused by the incomplete anodic regeneration of the products formed during the quiescent period of the repeating voltage sweep.

(*ii*) *Dependency on the head of mercury:* Another test for determining the reversibility of electrode reactions involves the dependency of the peak diffusion current on the head of mercury. According to equation 4 the peak current is proportional to the quantity $m^{2/3}t^{2/3}$. The effect of the height of mercury on m and t (52, page 70) is such that for reversible reactions the maximal peak height is independent of the height of mercury. The deviation of maximal peak current from a constant value as the head of mercury is increased or decreased is used as a criterion for the irreversibility of the electrode reaction. Depending on the ion reduced, the maximal peak current did not remain constant, but either increased or decreased when the head of mercury was increased; an increase in current was more frequently observed. Thallous ion in 0.5 M potassium nitrate and cadmium ion in 1 M potassium chloride, both known to react reversibly at the dropping mercury electrode in ordinary polarographic technique, showed only slight variations of maximal peak current with the height of the mercury head. For irreversible reactions, such as nickel ion in tetramethylammonium bromide solution and iodate ion in sodium hydroxide solution, variations of maximal peak current with the head of mercury were large. For zinc ion, the peak current wave was found to be practically independent of the mercury pressure, a result which is unexpected in view of the completely irreversible nature of the electrode process for that ion.

An explanation for the increase in maximal peak current as the head of mercury is increased for irreversible reactions has been given by Delahay and Perkins (17). The concentration of a reducible species about the electrode surface decreases from one potential sweep to another because the anodic dissolution process, together with the diffusion process, is not sufficiently rapid to maintain the concentration of the reacting species at the mercury surface the same as that in the bulk of the solution. When the head of mercury is increased, the drop-time decreases and consequently the number of voltage sweeps per drop

decreases for a given frequency. As a result, the decrease in the concentration of the reacting substance at the electrode surface is smaller when the head of mercury is increased; hence the maximal peak current increases.

On the other hand, a decrease in maximal peak current when the head of mercury is increased was explained by assuming that the concentration of the reacting species at the mercury surface is greater than that in the bulk of the solution. This increase in concentration takes place by a sudden dissolution of the reduced product at the surface of the mercury drop. As the head of mercury is increased, the number of voltage sweeps per drop decreases and the increase in the concentration at the electrode surface is smaller. The result is a decrease in maximal peak current as the head of mercury is increased.

(c) Symmetry of redox pattern

The method of Sevcik (74) for producing i–E curves (i.e., triangular voltage sweep) has the advantage of providing not only the reduction wave but also the oxidation wave, which is essential if a complete picture of the combined electrode processes is desired.

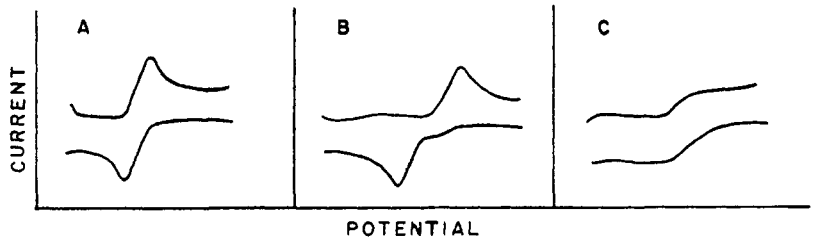

FIG. 15. Shape of current–potential oscillograms obtained with a triangular voltage sweep for: (A) the reversible reaction involving lead ion, (B) the irreversible reaction involving zinc ion, and (C) the retardation of the reaction of cadmium ion in the presence of gelatin.

For the case of i–E curves, Sevcik (74) has stated that the half-wave potential of the cathodic curve for an electrolytic process may be calculated by adding $40/n$ mv. to the potential at which the current is maximal, where n is the number of electrons transferred during the reduction process. The same amount is subtracted from the potential of the maximum of the anodic wave to find the half-wave potential of the anodic curve. If the two half-waves are identical, the electrode process is reversible; if not, the electrode process is irreversible. The curves due to the electrode process for thallium, lead, and cadmium ions were found from experimental oscillograms to proceed reversibly according to the foregoing calculation.

In view of the fact that the peak-current equation developed by Sevcik was based on the assumption that the Nernst equation holds for reversible systems, it would seem likely that the mid-point of the steep portions of the reduction and oxidation waves should occur at the same potential.

For a typically reversible reaction, lead ion in 1 N potassium hydroxide, an

oscillogram (74) is obtained at a sweep frequency of 20.8 cycles per second (figure 15A) where the oxidation and reduction half-wave curves occur at the same potentials. The zinc ion, reversible in classical polarography, is shown to be oscillographically irreversible (figure 15B). Sevcik has ascertained that the cathodic and anodic half-wave potentials for zinc ion in 1 *N* ammonium chloride–1 *N* ammonium hydroxide differ by about 0.22 v., the less negative value being that for the oxidized form. This difference was independent of the frequency of the potential sweep from 0.8 to 73 cycles per second. In the case where the reaction at the electrode proceeds slowly, diffusion is of minor importance and the limiting current is determined by the kinetics of the reaction. Thus, cadmium ion in 1 *N* hydrochloric acid plus gelatin, at 73.4 cycles per second (figure 15C), shows no peak but only a small rise in current in both branches. In the case of trivalent indium, the rate of electrodeposition of the ion was found to be much slower than that of the oxidation of the reduced form. The retardation of the rate of deposition of reducible ions in the presence of gelatin was easily observed. Gelatin had no effect on the redox behavior of monovalent thallium ion. For divalent cadmium both oxidation and reduction were influenced and for trivalent indium only the reduction was slowed.

2. Potential–time patterns

Thus far the discussion has been centered on results obtained with current–potential oscillograms. Heyrovsky has extensively investigated the reversibility-irreversibility of electrode reactions by means of potential–time curves (37, 38, 40, 41, 42, 43, 46).

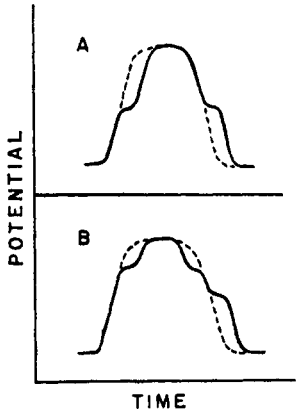

FIG. 16. Potential–time curves: (A) reversible reaction; (B) irreversible reaction

If the reaction is rapid and reversible, as in the case of cadmium, lead, or thallous ions in 1 *N* potassium chloride or nitric acid, the cathodic and anodic inflections occur at the same potential; this results in a symmetrical potential–time pattern (figure 16A). The dotted line marks the curve before the addition of the depolarizer. The width of the kink is a function of the concentration of the

depolarizer. If the reaction is irreversible, an unsymmetrical figure will occur, with the anodic kink appearing at a more positive potential than the cathodic kink. An example of this latter case is the reaction of zinc ion in potassium chloride, ammonium hydroxide, or potassium hydroxide solutions (figure 16B). Other divalent ions in the transition series give similar nonsymmetrical potential–time curves. Where the reaction at the electrode is so slow that no appreciable reduction occurs, no inflections are observed. This was noticed in the case of cadmium cyanide complex ion in 1 *N* potassium cyanide. There is a group of ions, including indium, bismuth, and antimony, which in solutions of certain anions—sulfate, nitrate, perchlorate, hydroxide, tartrate, and citrate—show definite oscillographic irreversibility, but which in an excess of chloride or bromide ion approach oscillographic reversibility and show an increased rate of electrodeposition.

(a) Zinc

Heyrovsky (41, 42) has discussed the reaction of zinc ion at the mercury electrode as a typical example of the irreversible reduction of the ions of the transition series in view of his findings with the *E–t* curves. His basic thesis is that the acceptance of more than one electron is not simultaneous but consecutive. The basis for this argument is that electrolytic processes involving the electrodeposition of bivalent ions, e.g., lead, are hindered by films such as that due to pyridine at the mercury surface (47). The reduction of lead ion proceeds freely only when the film breaks down. However, thallous ion, which requires only one electron for reduction, reacts reversibly, being unhindered by the film.

The first reaction in the reduction of zinc ion would be $Zn^{++} + e \rightarrow Zn^{+}$, where Zn^{+} is unstable. The potential required for this reaction is greater than that observed in ordinary polarography where the relatively slow process of adding two electrons can occur. The formation of Zn^{+} is then followed by either the disproportionation reaction of two Zn^{+} ions to give a Zn^{++} ion and metallic zinc, or the acceptance of another electron at the electrode to from metallic zinc. However, a second electron can be added only after rearrangement has taken place in the inner electron shell of the atom. On oxidation, zinc metal cannot part with two electrons at once, owing to a rearrangement within the electronic shell after the removal of the first electron. The process, $Zn \rightarrow Zn^{+} + e$, occurs at a more positive potential than is observed in the cathodic process. The Zn^{+} ion is then quickly converted into Zn^{++} ion, either by giving up a second electron to the electrode or by the dismutation reaction.

It has been supposed by Heyrovsky that the mercury cathode is charged so quickly that no deposition of zinc atom from divalent zinc ions can occur until the potential for the one-electron reduction is reached. For slow electrolysis the two-electron process occurs at a more positive potential. Therefore, at intermediate rates of voltage change one expects to find, according to this hypothesis, the reduction half-wave potentials for zinc ion to lie between that of the one-electron and that of the two-electron processes. According to Sevcik (74), however, the potential separation between the oxidation and reduction half-wave

potentials is independent of the frequency of the potential sweeps between 0.8 and 73 cycles per second, a result which is in contrast to this thesis. Further investigation into the phenomena of electrode reactions at the mercury electrode is required before there is complete substantiation of Heyrovsky's theory of reduction mechanisms. Until such is forthcoming, the theory proposed by Heyrovsky is a most useful one for understanding the irreversibility of many electrode processes.

(b) Effect of anions

The acceleration of irreversible reactions of indium and other trivalent cations by chloride and bromide ion is believed to be due to the ease with which these anions are deformed, e.g., polarized (41, 42). In a field of electric charge such as exists at the mercury electrode, the center of negative charge of the anion is shifted in a direction away from the electrode to a position closer to an incoming cation. Upon contact with the chloride ion the cation captures the electron and, simultaneously, an electron from the electrode replaces the lost charge on the chloride ion. Important is the fact that the influence of chloride ions was observed only for cathodic processes, the anodic kink being practically independent of the composition of the solution. This is in contrast to the observations of Randles (71), who found the rate at which zinc ions are formed from zinc amalgam in the presence of the nitrate, chloride, bromide, thiocyanate, and iodide ions to increase in the order given. Nickel and cobalt indicated similar increased rates of dissolution going from bromide to thiocyanate to iodide solutions. In this regard Doss and Agarwal (20) have shown mathematically, by consideration of the theory of absolute reaction rates, that the variations in the rate constant of the dissolution of zinc in various indifferent electrolytes can be interpreted on the basis of the variation of the equilibrium potential of the different systems.

On the other hand, Frumkin (24) suggested that the acceleration in rates may be attributed to a change in the structure of the double layer brought about by anion adsorption at the mercury surface. Notable is the fact that the irreversibility of the trivalent cations studied by Heyrovsky occurs in solutions of sulfate and nitrate ions, which are known not to be deformable in an electric field.

The effect of chloride ions on reduction processes is especially conspicuous in solutions containing divalent copper. In neutral or acid solution, two perfectly symmetrical kinks appear in the potential–time curve, due probably to the process $Cu^{+} + e \rightleftharpoons Cu$. The first step, which is not observed, occurs, according to Heyrovsky, at the potential of the calomel electrode, *viz.*, $Cu^{++} + e \rightleftharpoons Cu^{+}$. With the addition of ammonia, two more symmetrical steps appear, the potentials of the two single-electron steps having been shifted to more negative values. Asymmetric kinks are obtained for divalent copper in solutions containing sulfate, nitrate, chlorate, or hydroxide ion. For irreversible processes, an increase in temperature facilitates reversibility since at high temperatures, 80–90°C., the kinks on the potential–time patterns become more symmetrical.

Small amounts of ether, phenol, amyl alcohol, or isopropyl alcohol produced retardation effects in the reduction rates of metallic ions (39).

(c) Other cations

The observations of Heyrovsky that multivalent ions were sometimes reduced stepwise was confirmed by Prytz and Osterud (69) by oscillograms and polarograms of the perchlorates of lithium, sodium, thallium, lead, zinc, cadmium, and aluminum. With lithium, sodium, thallium, and lead, only one step was found. With zinc and cadmium, two separate waves were observed, one of which was at a more negative potential than usual. This is the first instance in which two waves have been recorded for the reduction of cadmium. In the case of aluminum, two steps were obtained at different potentials, apparently indicating that partial reduction precedes complete reduction.

Divalent ions, such as lead and cadmium, which are reversible oscillographically must dismutate extremely rapidly at the electrode. The fact that Delahay (16) found lead and cadmium to be slightly irreversible leads to the conclusion that the rates of the dismutation processes for these ions are finite.

Manganous ion in cyanide solution exhibits reversibility, the symmetrical kinks being due to the single-electron transfer, $Mn^{++} + e \rightleftharpoons Mn^{+}$. This process occurs at a more positive potential than that of the slower two-electron reaction. In other solutions manganous ion behaves irreversibly.

Data obtained with E–t oscillograms by Bieber and Trumpler (4) on manganous ion showed that in lithium chloride solution reduction occurred at a much more negative potential than oxidation. In fact, the reduction branch of the E–t curve indicated two kinks close together which the authors were not able to rationalize. In potassium chloride or zinc nitrate solution, only one reduction step was observed. In all cases the oxidation kink was much weaker than the reduction kink. This then is an example of the third category of irreversible reactions, where the oxidation occurs at a different potential from that of the reduction and one or more of the electrode processes is slow. In the case just cited the oxidation process is the slow step.

Experiments (4) with a streaming electrode on the same manganous solutions gave E–t patterns having symmetrical kinks on the reduction and oxidation branches of the curve; this indicates a reversible reaction. The kink which appears in the oxidation branch, however, is due solely to the cessation of reduction and is not truly an oxidation step.

(d) Organic compounds

The irreversible process for the reduction of nitroparaffins has been observed by Petru (67) with oscillographic potential–time curves. A cathodic kink is observed on the reduction branch, but there is no time-lag on the anodic branch for the oxidation of the reduction product of nitromethane. The derivative curve obtained with an acidic solution of equimolar concentrations of nitrobenzene and nitromethane indicates that the reduction slope for nitrobenzene is about four times steeper than the slope due to the reduction of the nitromethane.

This suggests the probability that all four electrons are acquired simultaneously by nitrobenzene, while the nitromethane accepts electrons successively. It should be pointed out that, according to classical polarographic wave analysis, the slope of the current–potential curve for the reduction of nitrobenzene indicates an n value of 1, while the height of the wave according to Ilkovic's equation shows a total transfer of four electrons (66). On this basis, the reduction process is irreversible and probably proceeds stepwise. Experiments with the streaming mercury electrode, where slow electrolytic processes give small, not too well-defined waves, showed a well-defined wave in the case of nitromethane, indicating no retardation in the reaction at the electrode by any slackened kinetic process. The end product for a four-electron reduction process of aliphatic nitro compounds has been shown by Seagers and Elving (73) to be the hydroxylamine.

Heyrovsky (42) has investigated the reversibility of several organic compounds by the E–t procedure and found that hydroquinone, formaldehyde, cystine, and picolinic acid gave perfectly symmetrical patterns. Those found to be irreversible were fumaric, maleic, nicotinic, and ascorbic acids, alkaloids, etc. A systematic study of the reversibility of such compounds, however, is yet to be made. The interpretation of such curves is not entirely clear, especially in view of Heyrovsky's concept of "polarographic irreversibility" (*cf.* Section V,B).

3. Current–time patterns

Bieber and Trumpler (5) utilized current–time oscillograms to study the kinetic character of the reduction of formaldehyde. Wiesner (79) was able to show by i–t curves registered on a cathode-ray oscilloscope that the reduction of certain sugars was kinetically controlled, since the current was proportional to $t^{2/3}$ rather than the diffusion-controlled process where current is a function of $t^{1/6}$.

The lowering of hydrogen overvoltage at the dropping mercury electrode by certain pyridine derivatives in buffered solution was studied by Knoblock (51). Oscillographic current–time curves, followed during the formation of each mercury drop, showed current maxima at the potentials at which the catalytic effect began; this indicated that an adsorption of the cations of the nitrogen base from buffered solution takes place.

Meites *et al.* (33) have discussed a current–time instrument capable of measuring current accurately to about 0.1 microamp. and the age of the mercury drop to ± 0.5 millisec. During the first few milliseconds of drop-life, the polarographic current shows a rapidly damped sine-wave-like variation. This phenomenon was found to be due to the vibrations of the surface of the mercury meniscus within the capillary, which in turn affected the area of the electrode–solution interface.

Current–time oscillograms were utilized by Antweiler (2) as a means of studying maxima formation and streaming of electrolytes about a mercury electrode surface. Irregularities in the current–time oscillograms were found to be closely associated with electrolyte streaming as determined by optical interference methods and with the production of maxima in current–potential polarograms.

Current passed by a dropping mercury electrode during the drop-life was observed oscillographically by Bon and Reboul (8, 9). The current was measured as a function of the height of the mercury head, the frequency of the mercury drops or life-time, the resistance in series with the dropping mercury electrode, the concentration of the solution, and the nature of the supporting electrolyte. From the shapes of the i–t oscillograms, studies on surface-active phenomena could be made. Very small amounts of oxygen gave rise to a sudden increase in current, the magnitude of which could be modified by suppressors. Traces of zinc, lead, or tin in mercury could be detected by this technique.

4. Alternating-current methods

Randles (71) has effectively studied electrode kinetics by applying a small alternating voltage to an electrode at which an electrochemical reaction is in equilibrium. The electrode process and diffusion phenomena were considered to be electrically equivalent to a capacitance and resistance in series. The measurement of the capacitance and resistance of the electrode process in terms of a phase angle enabled the rate constant for the electrode process to be determined. Ershler (21) has made alternating-current measurements of capacitance and conductance of an electrode in equilibrium with a solution at different frequencies, permitting the investigation of the kinetics of different electrode reactions. Breyer and Gutman (11) have discussed the behavior of reversible electrode reactions in alternating fields and have given the terms "dynamic capacitance" and "dynamic resistance" to the apparent capacitive and resistive features encountered during electrode processes. For reversible electrode reactions a capacitive component is observed, while for irreversible electrode reactions there is no indication of dynamic capacitance. Potentially, the alternating potential methods offer a valuable means of investigating the kinetics of electrode processes. As previously mentioned, Laitinen (54) has discussed oscillographic and alternating-current polarographic techniques as applied to electrode kinetics.

5. Summary of available data

Reactions which have been found reversible by the various oscillographic techniques are given in table 2. Such reactions have identical oxidation and reduction half-wave potentials as far as can be ascertained and the rates of the electrode processes are fairly rapid. The decision as to whether a reaction is rapid or slow was based on the comparison of the relative rates of reactions in two ways: (*1*) Where the rate of reaction of the same electroactive species is different in various base solutions, e.g., the rate of reduction of nickel ion proceeds more rapidly in thiocyanate solution than in chloride solution, the former reaction is considered rapid and the latter slow. (*2*) Where the rates of reaction of different electroactive species in the same supporting electrolyte vary widely, e.g., cadmium is reduced more rapidly than cobalt in chloride solution, the reaction of cadmium is considered to be rapid while that of cobalt to be slow.

Table 3 contains all the reactions investigated oscillographically which have shown irreversibility. In accordance with the present authors' views, each irre-

versible reaction is considered separately as to whether the difference in half-wave potential or the rate of reaction is the predominating observable factor controlling the process. Cases where both factors are discernible are also encountered. Unique is the fact that no single electrode processes have been found to be irreversible except where transfer of electrons is hindered by film formation. The two- and three-electron reductions and oxidations may be accomplished

TABLE 2

Reversible reactions

REDUCIBLE SPECIES	BASE SOLUTION	ELECTRODE REACTION
Na^+	Cl^-, OH^-	$Na^+ + e \leftrightharpoons Na$
K^+	Cl^-, OH^-	$K^+ + e \leftrightharpoons K$
Tl^+	Cl^-, OH^-	$Tl^+ + e \leftrightharpoons Tl$
Cu^+	Cl^-, NH_3	$Cu^+ + e \leftrightharpoons Cu$
U^{+6} *	Cl^-	$U^{+6} + e \leftrightharpoons U^{+5}$
Mn^{++}	CN^-	$Mn^{++} + e \leftrightharpoons Mn^+$
Cu^{++}	NH_3	$Cu^{++} + e \leftrightharpoons Cu^+$
Pb^{++}	Cl^-, CN^-, OH^-	$Pb^{++} + 2e \leftrightharpoons Pb$
Cd^{++}	Cl^-	$Cd^{++} + 2e \leftrightharpoons Cd$
Ni^{++}	CN^-	$Ni^{++} + 2e \leftrightharpoons Ni$
Co^{++}	CN^-	$Co^{++} + 2e \leftrightharpoons Co$
Sn^{++}	Cl^-	$Sn^{++} + 2e \leftrightharpoons Sn$
Fe^{+++} *	Cl^-	$Fe^{+++} + e \leftrightharpoons Fe^{++}$
Cr^{+++} *	Cl^-	$Cr^{+++} + e \leftrightharpoons Cr^{++}$
In^{+++}	Cl^-	$In^{+++} + 3e \leftrightharpoons In$
Sb^{+++}	Cl^-	$Sb^{+++} + 3e \leftrightharpoons Sb$
Bi^{+++}	Cl^-	$Bi^{+++} + 3e \leftrightharpoons Bi$
Formaldehyde	Buffer	Reversible product short-lived and transformed to an irreversible reduction product
Hydroquinone		
Cystine		
Picolinic acid		

* No direct information was available to confirm the use of a chloride base solution. However, since chloride ion enhances reversibility, it is assumed that this is probably the electrolyte used.

by a series of single-electron processes which in themselves are reversible, but the overall reaction may be irreversible.

C. MEASUREMENT OF RATES OF REACTION

Until recently, the contributions of oscillographic polarography as a tool for the study of the kinetics of chemical reactions have been largely limited to inorganic electrode reactions, as discussed in the preceding section. A recent paper by Snowden and Page (76) has emphasized the potentialities of the technique to the analysis of organic systems and especially to studies in the field of reaction kinetics. Rapid as well as slow rates of reaction may be measured whenever any of the reactants or products formed is electroactive. Moreover, short-lived

intermediates which are reducible may possibly be detected. Reactions which were studied by Snowden and Page were (*1*) relatively rapid, light-sensitive reactions involving diazo compounds, (*2*) thermal decomposition of diazonium

TABLE 3

Irreversible reactions

REDUCIBLE SPECIES	BASE SOLUTION	ELECTRODE REACTION	DIFFERENT CATHODIC AND ANODIC HALF-WAVE POTENTIALS	SLOW ELECTRODE PROCESS
H^+	Cl^-	$2H^+ + 2e = H_2$		x
Zn^{++}	Cl^-, NH_3	$Zn^{++} + 2e = Zn$	x	
Mn^{++}	Cl^-, NH_3	$Mn^{++} + 2e = Mn$	x	Anodic
Fe^{++}	Cl^-, NH_3	$Fe^{++} + 2e = Fe$	x	Anodic
Cd^{++}	CN^-	$Cd^{++} + 2e = Cd$		x
Sn^{++}	SO_4^{--}	$Sn^{++} + 2e = Sn$		x
Ni^{++}	$(CH_3)_4NBr$, CNS^-, Cl^-	$Ni^{++} + 2e = Ni$		Anodic
Co^{++}	CNS^-	$Co^{++} + 2e = Co$		x
Co^{++}	Cl^-	$Co^{++} + 2e = Co$		Anodic
Cr^{++}		$Cr^{++} + 2e = Cr$	x	
Ni^{++}	CNS^-	$Ni^{++} + 2e = Ni$		x
Cu^{++}	SO_4^{--}, NO_3^-, ClO_4^-, OH^-, tartrate, or citrate	$Cu^{++} + 2e = Cu$	x	
In^{+++}		$In^{+++} + 3e = In$	x	
Bi^{+++}		$Bi^{+++} + 3e = Bi$	x	
Sb^{+++}		$Sb^{+++} + 3e = Sb$	x	
Cr^{+++}	NH_3	$Cr^{+++} + 3e = Cr$	x	
In^{+++}	HCl	$In^{+++} + 3e = In$		Cathodic
Al^{+++}	LiCl	$Al^{+++} + 3e = Al$		Anodic
Ga^{+++}		$Ga^{+++} + 3e = Ga$		No cathodic wave
Eu^{+++}		$Eu^{+++} + e = Eu^{++}$		x
Ti^{+4}		$Ti^{+4} + e = Ti^{+++}$		x
IO_3^-	KOH H_2SO_4	$IO_3^- + 6e = I^-$		x
CH_3NO_2	Acetate buffer	$-NO_2 + 4e = -NHOH$		No anodic wave
$C_6H_5NO_2$	Acetate buffer	$-NO_2 + 4e = -NHOH$		No anodic wave
Phenylglyoxylic acid	pH 8			No anodic wave
Fumaric acid				
Maleic acid				
Nicotinic acid				
Ascorbic acid				
Alkaloids				

compounds, (*3*) formation of azo dyes by diazo-coupler reactions, and (*4*) reaction between formaldehyde and acetone in slightly basic media with the formation of 3-oxo-1-butanol. When diazonium compounds were exposed to ultraviolet radiant energy, the peak current was proportional to time, indicative of zero-order reactions.

The thermal decomposition of a diazo salt resulted in a first-order reaction plot of current (concentration) *vs.* time. The measurement of peak current with time for the formation of an azo dye by coupling gave data which fitted the second-order reaction formula. The ability of the cathode-ray polarograph to measure rates of reactions which go to completion in 30 sec. or more provides a tool for studying reactions which hitherto were too rapid to measure by other methods.

The applicability of the oscillographic technique to the determination of the kinetics of some heavy metal–nitrilotriacetic complexes was shown by Koryta and Kossler (53). The rates of formation and dissociation of the complexes were of such an order as to make impossible the evaluation of the half-wave potential displacement or the heights of the current waves for the reduction of free and complex ions, as long as the dropping mercury electrode was used. However, by using a streaming mercury electrode, where a rapid renewal of the diffusion layer at the electrode surface takes place, the kinetic contribution was eliminated and the stability constants determined. The (dE/dt)–E oscillograms observed distinguished between the kinetic contribution due to the slow rate of complex formation at the dropping mercury electrode and the suppression of the effect of dissociation of the complex in the case of the streaming mercury electrode.

D. CAPACITY PHENOMENA AND FILM FORMATIONS

The capacity of the electrical double layer at the mercury–solution interface has a pronounced effect on the current–potential pattern obtained in oscillographic work. The oscillographic observation of the capacitive properties of the interfacial region promises to be a most important tool for the investigation of film formation at the interface as well as for the nature of the electron-transfer process.

There has been some discussion concerning the resistance encountered at the electrode interface during a reaction (28). The largest value of polarization resistance for a dropping mercury electrode was calculated to be 0.075 ohm at 1000 cycles per second (28). This resistance, as well as the capacity of the double layer, was found to vary little with frequency. The results indicate that the dependency of resistance and capacitance on frequency is a function of the degree of polarizability of the electrodes used; the largest effect that frequency had on capacity was noticed with nonpolarized electrodes.

1. Differential capacity

The capacity current is directly proportional to the differential capacity of the electrical double layer at the electrode–solution interface and to the rate of the potential variation.

Ilkovic (48) measured the capacity of the electrical double layer for certain salt solutions, which he called the "polarization capacity." His results are in approximate agreement with values calculated by Grahame (31) and Gouy (25).

The most recent and most comprehensive investigation on differential capacity at the mercury electrode has been reported by Grahame (30). His method of

measuring the differential capacity of the electrical double layer with great accuracy at any potential involves the use of an impedance-type capacity bridge with a cathode-ray oscilloscope as a null-point indicator. A synchronized timing mechanism indicates the age of the mercury drop at the instant the null point is reached. From the age of the drop and the rate of flow of the mercury, the area of the drop is calculated.

Loveland and Elving (59) have applied the triangular sweep circuit to the determination of differential capacity (figure 17). On one arm of the voltage sweep the mercury electrode is charged, while on the other arm the electrode is discharged, resulting in two oscillographic traces. The symmetry of the two curves indicates the rapidity with which the electrical double layer is formed.

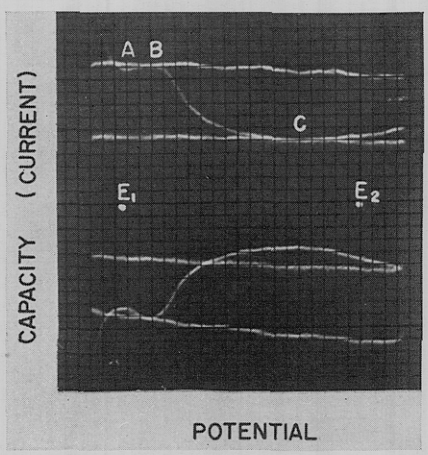

FIG. 17. Differential capacity-current oscillogram for 0.1 N magnesium chloride. $E_1 = -0.264$ v.; $E_2 = -1.559$ v.

By using known mercury drop areas and by comparing the differential capacity current with that obtained with a standard capacity, good agreement was obtained between observed and known minima for differential-capacity values at A and C, and between observed and known maximum values at B of figure 17.

Since the differential capacity is not constant with applied potential, the current–potential oscillograms should not be linear but vary directly with the capacity. On the basis of Grahame's data (29, page 462), Delahay (14) uses a value of 38 microfarads per square centimeter for the capacity of the double layer on the positive branch of the electrocapillary curve and 18 microfarads per square centimeter for the capacity on the negative branch for a 0.5 M sodium sulfate solution. With these values of capacity, he calculated the capacity current that is expected for the positive and negative branches of the electrocapillary curve; the observed and caclulated values differed by 12 and 17 per cent, respectively.

In the presence of a small amount of reversibly reducible substance, the apparent capacity of the mercury electrode is enormously increased in the neigh-

borhood of the half-wave potential; this increase is designated as a "pseudo-capacity" (29). The capacity is increased because the reduced form of the ion acts as a reservoir of charge. When there is no more change in concentration of the reduced form of the ion, the differential capacity becomes normal (figure 18).

The characteristics of the differential capacity curves depend greatly upon the anion present in solution and almost not at all on the cation (29). Humps appearing near the electrocapillary maximum of most curves are believed to arise from mutual electrostatic repulsion of ions in the double layer in directions parallel to the interface. According to Grahame (29), a 1 sq. cm. mercury surface in a solution of 1 M sodium chloride exhibits an apparent resistance (polarization resistance) of less than 0.02 ohm. The capacity is about 18 microfarads per square centimeter and therefore the time constant of the combination, RC, is 3.6×10^{-7} sec. This indicates that the time required to establish ionic equilib-

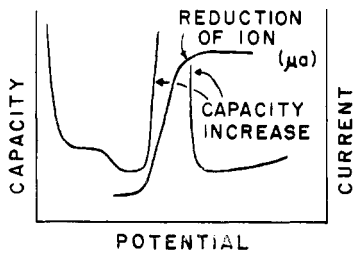

FIG. 18

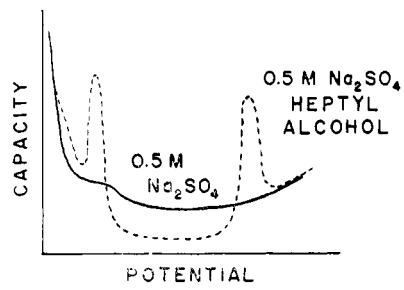

FIG. 19

FIG. 18. Influence of the presence of a reducible ion on the differential capacity of the electrical double layer.

FIG. 19. Influence of the presence of a nonelectrolyte on the differential capacity of the electrical double layer.

rium is a microsecond or less. In actual practice, the resistance of the solution and the capacitance between the electrodes will delay the attainment of equilibrium to a small extent depending on the RC product of the two values. Sevcik (74) has illustrated an i–E pattern due to the charging and discharging capacity-current curves for a 1 N potassium hydroxide solution.

Indirect measurements, involving the use of a cathode-ray oscilloscope, of the capacity of the electrical double layer of a mercury electrode were carried out by Fedotov (22). In essence, the potential at a mercury cathode is measured immediately after a polarization current of about 1×10^{-4} amp. per square centimeter is cut off. The method involves the photographic recording of this potential as a function of time as observed with a cathode-ray oscilloscope. The potential and time scales on the photograph are determined by recording, respectively, the discharge of a calibrated capacitor and a 10,000-c.p.s. A.C. signal. The oscillograms show that the potential decreases linearly with time for cases where the current density at time equal to zero is less than 4×10^{-4} amp. per square centimeter. The capacity is calculated from the equation, $C\ dE = i_0 t$, where C is the capacity, dE is the change of potential, and i_0 is the current

density when time, t, is zero. When current densities are greater than 4×10^{-4} amp. per square centimeter, a modified equation is required.

(a) Effect of film formation

(*i*) *Current–potential trace:* The differential capacity (29) of the double layer between the mercury and aqueous 0.5 M sodium sulfate solution with and without the addition of *n*-heptyl alcohol is shown in figure 19. The two large increases in the differential capacity appearing at low and high negative potentials due to the presence of heptyl alcohol in the sodium sulfate solution is of particular interest because of Heyrovsky's (35) work on capacity phenomena where he observed two kinks in each branch of the potential–time curve for higher alcohols in a sulfuric acid medium. In all probability, the potential–time curve

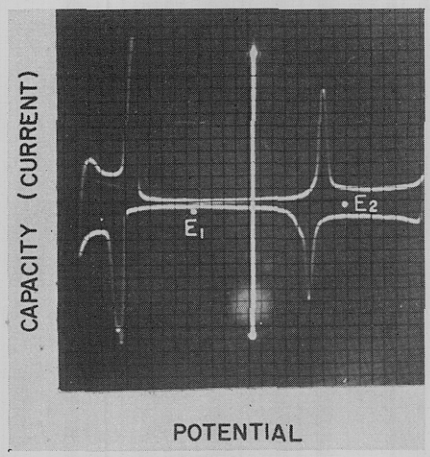

FIG. 20. Capacity effects of octyl alcohol in 0.5 M sodium sulfate. $E_1 = -0.300$ v.; $E_2 = -1.240$ v.

for the 0.5 M sodium sulfate–heptyl alcohol would consist of two kinks in the cathodic branch and two corresponding kinks in the anodic branch. The kink at the less negative potential on the charging branch would indicate the formation of a film, while that at the more negative potential would correspond to the breaking of the film at the electrode. On discharging, the most negative kink corresponds to the formation of a film and the least negative kink to the desorption of the film layer. This phenomenon of alcohol film formation has been nicely observed in i–E curves by Loveland and Elving (59). The charging and discharging adsorption i–E capacity patterns for octyl alcohol in 0.5 M sodium sulfate solution (figure 20) are almost identical with that illustrated in figure 19.

(*ii*) *Potential–time trace:* It was mentioned previously that a time-lag in the potential–time curves could be produced by either a depolarization reaction or a change in capacity. Heyrovsky *et al.* (47) have studied the capacity effects at the mercury electrode produced by indifferent substances in solution. Pyridine is not reduced in alkaline solution using the ordinary polarographic apparatus.

yet a well-defined, symmetrical time-lag appears at about −1.5 v. on the potential–time curve (figure 21). This phenomenon can only be explained by a sudden change in the capacity of the mercury electrode.

At point *A* in figure 21 an increase in capacity takes place corresponding to a desorption process, while at *B* a decrease in capacity occurs, corresponding to the adsorption of a pyridine film at the electrode. There is no doubt that this time-lag is due to capacity changes, since the concentration of pyridine required to produce this time-lag is about 100 times as large as that required to produce a similar kink in the potential–time curve for an electrolytic depolarizer. The derivative curve, (dE/dt)–t, for figure 21 shows sharper discontinuities in the anodic branch *B* than in the cathodic branch *A*. This indicates that the desorption process is slower and more gradual than the adsorption process. The potential at which the two processes occur was exactly measurable by ordinary

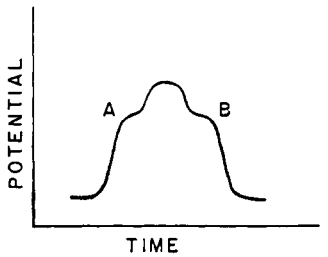

FIG. 21. Potential–time relationship obtained with pyridine in base solution

polarographic methods and was interpreted to be the breakdown potential of a condenser containing oriented pyridine molecules as a dielectric.

Similar adsorption–desorption effects were obtained with nitrogen bases in alkaline solution, with butyric acid in acid solution, and with ethyl ether, benzene, menthol, butyl alcohol, and ethyl bromide in solutions at any pH. Methyl and ethyl alcohols, propionic and acetic acids, and glycerol showed no effect.

Capacity effects are visible at a frequency of 8000 cycles per second, indicating that the film layer is rebuilt very rapidly.

The derivative curve $(dE/dt$–$t)$ has been used to determine the ratio of the capacity of the film to that of the aqueous double layer. The current which passes through the fixed capacitor C (figure 6) and is measured on the ordinate is inversely proportional to the capacity of the double layer at the mercury electrode. In the case of pyridine it was estimated that the ratio of the capacity of the solution without pyridine to that with pyridine was about 2 to 1. More accurate methods are available for determining such capacity ratios by determining separately the differential capacity of the base solution and then the solution containing the adsorbed material by techniques which have been described by others (30, 59).

(*iii*) *Current–time trace:* Adsorption phenomena for certain reducible compounds or their reduction products at the dropping mercury electrode have been studied by observing oscillographically current–time relationships for in-

dividual mercury drops (10, 80). When adsorption takes place at constant applied potential, the current is no longer proportional to the one-sixth power of the time. Instead, one or more maxima are present, occurring any time from the beginning of the drop to the end of the drop, depending on the substance present and the potential applied. Each maximum corresponds to a different adsorption process. The concentration of the adsorbable species alters the shape of the current–time relationship and at sufficiently low concentrations the adsorption effect is negligible. It is possible, in many cases, to ascribe each maximum to the adsorption of a particular reducible or reduced species or even intermediate at the mercury surface. Information of this nature is valuable for understanding the irreversible nature of many organic oxidation–reduction processes at the mercury electrode. Thus, Brdicka (10) was able to point out in the reduction of lactoflavin the existence of the leuco form as a reduction product and the semiquinone as an intermediate.

2. Surface charge density

Oscillograms of differential capacity current may be electronically integrated to give oscillographic patterns of surface charge density (60). The accuracy obtainable by this method is good when values of surface charge density obtained are compared to those from graphical integration of differential capacity values (31). The time required is a fraction of that required for graphical integration. Figure 22 illustrates a typical oscillographic surface charge density pattern for a 0.1 N lithium chloride solution. The oscillograms are obtained at a known area of a mercury drop. The calibration of the surface charge density axis is accomplished by electronic integration of the capacity current obtained from a standard capacity under the same voltage sweep conditions as used with the dropping mercury electrode. The vertical distance between the ends of the calibration line is proportional to the charge of the standard capacity, which is given as

$$Q_c = VC_c \tag{28}$$

where Q_c is in microcoulombs, C_c is in microfarads, and V is the potential span of the sweep used.

The potential of zero charge cannot be determined directly from the observed pattern. However, several methods are available for finding this potential (32) and data for several solutions are available in the literature (32, 52). The effect of film formation on the shape of the surface charge density pattern is illustrated in figure 23, which has been obtained by the integration of the capacity-current curve of figure 20. Points A and B of figure 23 correspond to the potentials of the adsorption and desorption processes of the alcohol layer at the dropping mercury electrode. The flat portion between A and B corresponds to a small increase in surface charge density, which is a result of the adsorption of a film of alcohol about the mercury surface. At potentials more positive than A and more negative than B, the surface charge density curve becomes normal.

3. Surface tension–electrocapillary curve

The applicability of oscillographic techniques to the determination of the electrocapillary curve has been indicated by Loveland and Elving (60). By performing a double electronic integration on the pattern of the differential capacity current, the surface tension *vs.* potential curve may be obtained. The distinct advantage of observing the electrocapillary curve on the face of an oscilloscope is that a complete pattern is obtained for each mercury drop during the lifetime of a drop.

Studies of surface-active substances may be made by observing the shape of the electrocapillary curve; e.g., the effects of numerous organic nonelectrolytes

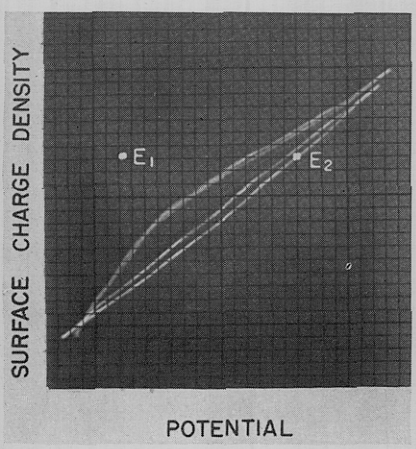

FIG. 22

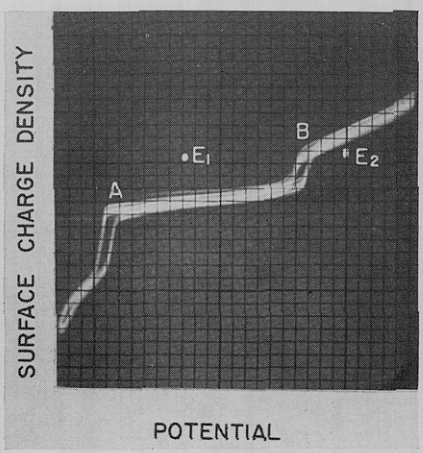

FIG. 23

FIG. 22. Surface charge density relation for 0.1 *N* lithium chloride. $E_1 = -0.488$ v.; $E_2 = -1.538$ v.

FIG. 23. Effect of octyl alcohol on the surface charge relation of 0.5 *M* sodium sulfate. $E_1 = -0.336$ v.; $E_2 = -1.305$ v.

on the shape of the electrocapillary curve were observed by Gouy (26, 27) at an early date. However, such effects are more adequately studied by means of the curve for the differential capacity current or that for the surface charge density (59, 60), since any small change in the electrocapillary or surface-tension curve is accentuated in the curves which are its first and second derivatives.

VI. SUMMARY

Since 1946 there has been considerable investigation of the phenomena at mercury electrodes, using cathode-ray oscillographic observation to obtain instantaneous patterns of the relation between two variables. These variables are associated with the electrical properties of the electroactive species in solution, and the external electrical and electronic devices. Circuit arrangements have been designed for obtaining current–potential, potential–time, current–time, and first derivatives of some of the foregoing. The results and data obtained are

intimately related to conventional polarographic techniques involving current–potential relationships at a polarized microelectrode. In oscillographic polarography the current–potential waves are characterized by diffusion currents with peaks.

Where charging and discharging potential sweeps are employed, comparison of the resulting anodic and cathodic waves serves to indicate the degree of reversibility as well as the relative rates of the electrode processes. Oscillographic methods are well adapted to obtaining qualitative and quantitative data, as well as to the investigation of the kinetics of chemical reactions when one or more of the reactants or products are electroactive under the experimental conditions. The subject of the reversibility-irreversibility of electrode reactions can be investigated.

Capacity currents observed with certain current–potential circuits can be used to give information concerning the differential capacity and surface charge density relations in the interfacial region. The phenomena of film formation due to the adsorption–desorption of nonelectrolytes at the surface of a mercury electrode, which results in capacitive charges, can be readily followed.

Both diffusion-current and capacity-current phenomena have been treated in a mathematical manner; the shortcomings and experimental consequences of the derived equations can be predicted.

The current–time, current–potential, and potential–time methods of oscillographic observation of phenomena at stationary, dropping, and streaming mercury electrodes have demonstrated their value for investigating adsorption and redox phenomena, and should in the future be of great significance as a means of clarifying some of the multitudinous problems prevalent in the field of electrode mechanisms and kinetics.

The authors wish to express their gratitude to the Office of Naval Research for supporting the research project upon which this review was prepared.

VII. References

(1) Airey, L.: Analyst **72,** 304 (1947).
(2) Antweiler, H. J.: Z. Elektrochem. **44,** 888 (1938).
(3) Bernheim, P., and Fournier, M.: Compt. rend. **230,** 297 (1950).
(4) Bieber, R., and Trumpler, G.: Helv. Chim. Acta **30,** 971 (1947).
(5) Beiber, R., and Trumpler, G.: Helv. Chim. Acta **30,** 1109 (1947).
(6) Boeke, J., and Suchtelen, H. van: Z. Elektrochem. **45,** 753 (1939).
(7) Boeke, J., and Suchtelen, H. van: Philips Tech. Rev. **4,** 231 (1939).
(8) Bon, F.: Compt. rend. **222,** 286 (1946).
(9) Bon, F., and Reboul, G.: Compt. rend. **224,** 1263 (1947).
(10) Brdicka, R.: Collection Czechoslov. Chem. Commun. **12,** 522 (1947).
(11) Breyer, B., and Gutman, F.: Faraday Society Discussions **1,** 19 (1947).
(12) Breyer, B., Gutman, F., and Hacobian, S.: Australian J. Sci. Research, **3,** 558 (1950).
(13) Breyer, B., Gutman, F., and Hacobian, S.: Australian J. Sci. Research **3,** 567 (1950).
(14) Delahay, P.: J. Phys. & Colloid Chem. **53,** 1279 (1949).
(15) Delahay, P.: J. Phys. & Colloid Chem. **54,** 402 (1950).
(16) Delahay, P.: J. Phys. & Colloid Chem. **54,** 630 (1950).

(17) DELAHAY, P., AND PERKINS, G.: J. Phys. & Colloid Chem. **55,** 586 (1951).
(18) DELAHAY, P., AND PERKINS, G.: J. Phys. & Colloid Chem. **55,** 1146 (1951).
(19) DELAHAY, P., AND STIEHL, G. L.: J. Phys. & Colloid Chem. **55,** 570 (1951).
(20) DOSS, K. S. G., AND AGARWAL, H. P.: J. Phys. & Colloid Chem. **54,** 804 (1950).
(21) ERSHLER, B. V.: Faraday Society Discussions **1,** 269 (1947).
(22) FEDOTOV, N. A.: J. Phys. Chem. (U.S.S.R.) **25,** 3 (1951); Chem. Abstracts **45,** 6095 (1951).
(23) FOURNIER, M., AND QUINTIN, M.: Compt. rend. **232,** 834 (1951).
(24) FRUMKIN, A. H.: Faraday Society Discussions **1,** 224 (1947).
(25) GOUY, G.: Ann. chim. phys. [7] **29,** 145 (1903).
(26) GOUY, G.: Ann. chim. phys. [8] **8,** 291 (1906).
(27) GOUY, G.: Ann. chim. phys. [8] **9,** 75 (1906).
(28) GRAHAME, D. C.: J. Am. Chem. Soc. **68,** 301 (1946).
(29) GRAHAME, D. C.: Chem. Revs. **41,** 441 (1947).
(30) GRAHAME, D. C.: J. Am. Chem. Soc. **71,** 2975 (1949).
(31) GRAHAME, D. C.: Office of Naval Research Project No. NR-051-150, Technical Report No. 1, 1950.
(32) GRAHAME, D. C., LARSEN, R. P., AND POTH, M. A.: J. Am. Chem. Soc. **71,** 2978 (1949).
(33) GRANT, D. W., MEITES, L., AND STURTEVANT, J. M.: Paper presented at the 120th Meeting of the American Chemical Society, New York, September, 1951.
(34) HEYROVSKY, J.: Chem. Listy **35,** 155 (1941).
(35) HEYROVSKY, J.: *Polarographie.* Springer Verlag, Vienna (1941).
(36) HEYROVSKY, J.: Metallwirtschaft **23,** 333 (1944).
(37) HEYROVSKY, J.: Chem. Listy **40,** 61 (1946).
(38) HEYROVSKY, J.: Chem. Listy **40,** 222 (1946).
(39) HEYROVSKY, J.: Chem. Listy **40,** 229 (1946).
(40) HEYROVSKY, J.: Analyst **72,** 229 (1947).
(41) HEYROVSKY, J.: Faraday Society Discussions **1,** 212 (1947).
(42) HEYROVSKY, J.: Wien. Chem.-Ztg. **48,** 24 (1947).
(43) HEYROVSKY, J.: Proc. Intern. Congr. Pure and Applied Chem. (London) **11,** 481 (1947); Chem. Abstracts **44,** 5757 (1950).
(44) HEYROVSKY, J.: Anal. Chim. Acta **2,** 533 (1948).
(45) HEYROVSKY, J.: Chem. Listy **43,** 149 (1949).
(46) HEYROVSKY, J., AND FOREJT, J.: Z. physik. Chem. **193,** 77 (1943).
(47) HEYROVSKY, J., SORM, F., AND FOREJT, J.: Collection Czechoslov. Chem. Communs. **12,** 11 (1947).
(48) ILKOVIC, D.: Collection Czechoslov. Chem. Communs. **8,** 170 (1936).
(49) JONES, T. S. G.: Electronics **16,** No. 4, 154 (1943).
(50) JONES, T. S. G.: Electronic Engineering **15,** 367 (1943).
(51) KNOBLOCH, E.: Collection Czechoslov. Chem. Communs. **12,** 407 (1947).
(52) KOLTHOFF, I. M., AND LINGANE, J. J.: *Polarography.* Interscience Publishers, Inc., New York (1940).
(53) KORYTA, J., AND KOSSLER, I.: Collection Czechoslov. Chem. Communs. **15,** 241 (1950).
(54) LAITINEN, H. A.: Ann. Rev. Phys. Chem. **1,** 309 (1950).
(55) LEEDS & NORTHRUP CO.: *Bibliography of Polarographic Literature,* Philadelphia (1950); Proceedings of the First International Polarographic Congress, Part II—*Polarographic Bibliography*, Prague (1951).
(56) LINGANE, J. J.: Anal. Chem. **21,** 45 (1949).
(57) LINGANE, J. J.: Anal. Chem. **23,** 86 (1951).
(58) LINGANE, J. J., AND LOVERIDGE, B. A.: J. Am. Chem. Soc. **72,** 328 (1950).
(59) LOVELAND, J. W., AND ELVING, P. J.: J. Phys. Chem. **56,** 250 (1952).
(60) LOVELAND, J. W., AND ELVING, P. J.: J. Phys. Chem. **56,** 255 (1952).
(61) MATHESON, L. A., AND NICHOLS, N.: Trans. Electrochem. Soc. **73,** 193 (1938).
(62) MCKENZIE, H. A.: J. Am. Chem. Soc. **70,** 3147 (1948).

(63) MEITES, L., AND MEITES, T.: J. Am. Chem. Soc. **72,** 4843 (1950).
(64) MÜLLER, R. H., GARMAN, R. L., DROZ, M. E., AND PETRAS, J.: Ind. Eng. Chem., Anal. Ed. **10,** 339 (1938).
(65) O'KELLEY, G. D., AND WILCOX, H. E.: J. Alabama Acad. Sci. **19,** 10 (1947).
(66) PEARSON, J.: Trans. Faraday Soc. **44,** 683 (1948).
(67) PETRU, F.: Collection Czechoslov. Chem. Communs. **12,** 620 (1947).
(68) PRYTZ, M., AND OSTERUD, T.: Tids. Kjemi Bergvesen Met. **1,** 27 (1941).
(69) PRYTZ, M., AND OSTERUD, T.: Arch. Math. Naturvidenskab **45,** 71 (1942).
(70) RANDLES, J. E. B.: Analyst **72,** 301 (1947).
(71) RANDLES, J. E. B.: Faraday Society Discussions **1,** 11 (1947).
(72) RANDLES, J. E. B.: Trans. Faraday Soc. **44,** 322, 327 (1948).
(73) SEAGERS, W. J., AND ELVING, P. J.: J. Am. Chem. Soc. **72,** 3241 (1950).
(74) SEVCIK, A.: Collection Czechoslov. Chem. Communs. **13,** 349 (1948).
(75) SMITH, G. S.: Nature **163,** 290 (1949).
(76) SNOWDEN, F. C., AND PAGE, H. T.: Anal. Chem. **22,** 969 (1950).
(77) STREHLOW, H., AND STACKELBERG, J. v.: Z. Elektrochem. **54,** 51 (1950).
(78) TAYLOR, J. K., SMITH, R. E., AND COOTER, I. L.: J. Research Natl. Bur. Standards **42,** 287 (1949).
(79) WIESNER, K.: Collection Czechoslov. Chem. Communs. **12,** 64 (1947).
(80) WIESNER, K.: Collection Czechoslov. Chem. Communs. **12,** 594 (1947).